

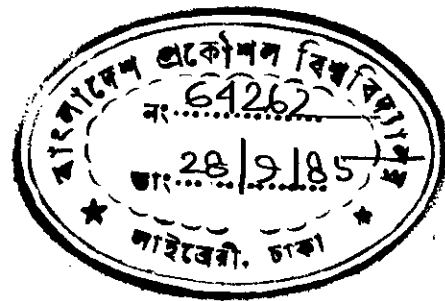
ANALYSIS OF NON-RECTANGULAR HIGH-RISE
TUBULAR STRUCTURES

A Thesis

By

A.K.M. ZUBAIR

Submitted to the Department of Civil Engineering,
Bangladesh University of Engineering and Technology, Dhaka
in partial fulfilment of the requirement for the degree
of
MASTER OF SCIENCE IN CIVIL ENGINEERING



September, 1985

821
1985
AKM



#64262#

ANALYSIS OF NON-RECTANGULAR HIGH-RISE
TUBULAR STRUCTURES

A Thesis
by
A.K.M. ZUBAIR

Approved as to style and content by:



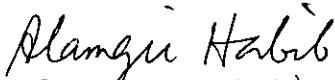
(Dr. J.R. Choudhury)
Professor of Civil Engineering,
and Dean Faculty of Civil Engg.,
BUET, Dhaka.

Chairman



(Dr. Shamim Z. Bosunia)
Professor and Head,
Dept. of Civil Engineering,
BUET, Dhaka.

Member



(Dr. Alamgir Habib)
Professor of Civil Engineering,
BUET, Dhaka.

Member



(Mr. M.A. Mannan)
Managing Director,
ASEA Consultants,
House No. 55C
Road No. 9A, Dhanmondaï,
Dhaka.

Member
(External)

September, 1985

ACKNOWLEDGEMENT

The author wishes to express his heartiest gratitude and profound indebtedness to Professor Jamilur Reza Choudhury for his supervision, guidance and encouragement at all stages of the present work. Without his constant guidance and invaluable suggestions at every stage, this work could not possibly have materialized.

Sincere thanks are due to Dr. Alamgir Habib, Professor of Civil Engineering and Dr. Shamim Z. Bosunia, Professor and Head of Civil Engineering for their encouragement and suggestions.

Sincere thanks are also due to Mr. A.K.M. Riazul Zamil, Mr. Rezaul Karim, Mr. Tariq Ahmed, Mr. H.M.R. Awal and Mr. Shamim Ahsan, with whom the author had many a fruitful discussion.

Gratitude is also expressed to computer centre staff for their co-operation in ensuring a fast turnaround of jobs submitted. The assistance of Mr. M.A. Malek and Mr. Shahiduddin in preparing the thesis is gratefully acknowledged.

ABSTRACT

A simplified method of analysis is developed for high-rise tubular structures of arbitrary plan shape, subjected to horizontal loading. Bari and Choudhury have recently (1984) developed a simplified method for analyzing high-rise tubular structures rectangular in plan, which is an extension of the continuous medium method proposed earlier by Coull and Choudhury (1967) for plane shear walls with multiple bands of opening. The method presented in this thesis extends the applicability of the method to tubular structures of arbitrary plan shape.

In this method, the analysis of deflections and stresses in a tubular structure is based on an idealization of the discrete system of connections formed by spandrel beams as an equivalent continuous medium with equivalent stiffness properties. Based on this simplified method, a computer program is developed in FORTRAN for determination of lateral deflection at top, column axial forces and girder bending moments produced due to point load at the top and lateral load uniformly distributed throughout the height.

A general computer program for space frame analysis is used to investigate the accuracy of the method of analysis. The applicability of the method is demonstrated by analyzing a 20-storied building, hexagonal in plan. The deflections and axial forces in columns of the tubular structure are studied

for buildings with different studied for buildings with different stiffness factors (S'_{f10}) of 0.1, 1.0 and 10.0. These results are compared with those obtained from a space frame analysis.

The results obtained from the proposed continuous medium method, in general, agree well with those obtained from the 'exact' method. The method can be used for any shape of structure by only changing the data for the geometry of structure. The computer program based on the method requires a very small computer storage and can yield acceptable results with very little computing effort. Therefore, the method can be conveniently used to rapidly evaluate the deflections and stresses for the tubular high-rise structures of any shape during preliminary design.

NOTATIONS

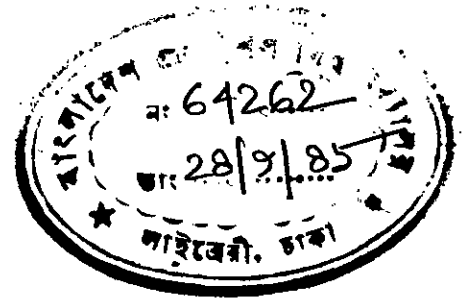
b	clear span of connecting beam
d	depth of connecting beam
H	building height
h	storey height
i, j, k	integer variables
$l_{x,i}, a_i$	distance between centroidal axes of the two walls/columns in x-direction
$l_{y,i}, c_i$	distance between centroidal axes of the two walls/columns in y-direction
n	number of walls or opening
q	shear force intensity in connecting medium
w_x	intensity of applied horizontal loading in x-direction
w_y	intensity of applied horizontal loading in y-direction
z	vertical distance of any section from top
Y_1	horizontal deflection in x-direction
Y_2	horizontal deflection in y-direction
A_i	cross-sectional area of ith wall
E	modulus of elasticity
G	shear modulus
$I_{x,i}$	moment of inertia of ith wall about x-axis
$I_{y,i}$	moment of inertia of ith wall about y-axis
$I_{p,i}$	moment of inertia of ith connecting beam
I_{ci}	reduced moment of inertia of ith connecting beam

T integral shear force
T' dT/dx ; $T'' = d^2T/dx^2$
 F_i axial force in i th wall
 U_1 strain energy due to bending of beam
 U_2 strain energy due to axial force of wall
 U_3 strain energy due to bending of walls
U total strain energy of the tube
 M_x bending moment in wall about x-axis
 M_y bending moment in wall about y-axis
 ν Poisson's ratio

CONTENTS

	Page
ACKNOWLEDGEMENT	
ABSTRACT	
NOTATIONS	
Chapter 1 INTRODUCTION	
1.1 General	1
1.2 Lateral Load Resisting System	3
1.3 Tubular System	4
1.4 Objective of the Thesis	17
Chapter 2 REVIEW OF AVAILABLE APPROXIMATE METHODS OF ANALYSIS OF TUBULAR STRUCTURES	
2.1 Introduction	18
2.2 Research on Shear-lag Analysis of Box Beams	18
2.3 Works on Rigid-tube Structures	20
Chapter 3 SIMPLIFIED ANALYSIS OF TUBULAR STRUCTURE OF NON-RECTANGULAR SHAPE BY CONTINUOUS MEDIUM METHOD	
3.1 Introduction	25
3.2 Assumptions	25
3.3 General Formulation	26
3.4 Computer Program	42
3.5 Modification for non-rectangular Shape	42
Chapter 4 RESULTS AND DISCUSSIONS	
4.1 Introduction	44
4.2 Results Obtained by Continuous Medium Method	46

	Page
4.3 Comparison between Continuous Medium Method and 3-D Space Frame Method	46
4.4 Discussion on Shear-lag Effect on Tubular Structure	50
Chapter 5 CONCLUSION AND RECOMMENDATION FOR FURTHER STUDY	
5.1 Conclusion	68
5.2 Recommendation for Further Study	69
REFERENCES	70
APPENDIX-A THREE DIMENSIONAL ANALYSIS OF SHEAR WALL	
A.1 Introduction	72
A.2 One-storey Structure	73
APPENDIX-B SPACE FRAME PROGRAM	
B.1 Introduction	81
B.2 Numbering Scheme	81
B.3 Member Load Sign Convention	82
B.4 Preparation of Input Data	89



1.1 General

High-rise buildings are closely related to the city - they are a natural response to dense population concentration, scarcity of land and high land costs. The modern trend in urban planning is to build high-rise buildings in developing cities, particularly for office buildings. Low-rise buildings are often replaced by taller blocks in the more developed areas. The economy, beauty, efficiency and above all the prestige associated with tall buildings have, in recent years, increased their rate of construction all over the world. The massing of highrise building evolves out of the designer's interpretation of the environmental context and his response to the purpose of building. However the tall buildings of the future may very well be an integral part of one large building organism, the city where the building or activity cells are interconnected by multi-level movement systems. High-rise buildings range in height from below 10 to more than 100 stories.

It is only in the last 30 years that reinforced concrete has found increasing use in the construction of tall buildings. In its initial development in the early parts of the twentieth century, reinforced concrete buildings were limited to only a few stories in height. The structural type used was the traditional beam-column frame system which made the construction of taller buildings relatively expensive. In the early 1950's,

the introduction of shear walls opened up the possibility of using concrete in apartment and office buildings as high as 30 stories. The taller buildings remain economically unattractive because the shear walls, which were mostly used in the core of the building, were relatively small in dimension compared to the height of such buildings, leading to insufficient stiffness to resist lateral loads. It was obvious that the overall dimensions of the interior cores were too small to economically provide the stability and stiffness for buildings over 30 to 40 stories.

The natural tendency then was to find new systems of structures that would utilize the perimeter configurations of such buildings rather than to rely on the core configurations alone. The development of the spatial wall frame, i.e., perforated wall structure known as rigid-tube was, therefore a logical out come of this challenge. The modifications of the rigid tube system into a tube-in-tube, framed tube and other variations are indeed known to offer certain advantage in planning, design and construction.

The rigid tube system usually relies on 'hull-core' i.e. tube-in-tube, type configurations for its basic layout: this has formed the structural backbone of almost all the tallest buildings constructed in recent years. The exterior enclosure tube or 'hull' usually consists of closely spaced columns connected together with deep spandrel beam at each floor level to form a multi-story multi-bay box frame. For apartment

buildings this hull tube alone or the hull with cross-walls provides the necessary stiffness against lateral loads. For office buildings, the external hull is usually combined with an internal service 'core' through the floor systems. The resulting 'hull-core' system is extremely efficient in resisting all kinds of horizontal loads viz. winds, earthquakes or blasts.

1.2 Lateral Load Resisting System

From a structural engineering stand point, one of the major distinguishing characteristics of a tall building is the need to resist large lateral forces due to wind or earthquake. The lateral load resisting system must conform with architectural, structural and mechanical schemes or vice versa. A lateral systems generally considered to be efficient if the provision of the lateral load resistance does not increase floor and column sizes beyond those required for gravity loads.

Although there are as many concepts of structural system to resist lateral load as there are designers, it is possible to classify these systems into categories. Each category to be most efficient for a certain height range or a certain type of occupancy. The most common framing systems are given below⁽¹⁷⁾.

- 1) The bearing wall structure.
- 2) The shear core structure.

- 3) Rigid frame systems.
- 4) The wall-beam structures: Interspatial and staggered truss systems.
- 5) Frame-shear wall building system.
- 6) Flat slab building structures.
- 7) Shear wall - Frame interaction system with rigid belt truss.
- 8) Tubular system.
- 9) Composite building.

1.3 Tubular System

A recent development in structural design is the concept of tubular behavior introduced by F.R. Khan⁽¹⁴⁾. At present, four of the world's five tallest buildings use the tubular system. They are, the John Hancock Building, the Shear's Tower, and the Standard Oil Building at Chicago and World Trade Center in New York (Fig. 1.1 e,h,g,f) respectively. Tubular system is so efficient that in most cases the amount of structural material used per square foot of floor space is comparable to that used in conventionally framed buildings half the size⁽¹⁷⁾.

The tubular system describes a structural system in which the perimeter of the building acts as a vertical, internally stiffened tube, resisting the horizontal forces from wind or earthquake. Since the exterior walls resist all or most of the wind loads, costly interior diagonal bracing or shear walls are eliminated. The rigidity of the tube is so high that it responds

to lateral loading similar to a cantilever beam.

Deflection of the tube in a very tall building consist of the 'chord' drift caused by the shortening and lengthening of the column elements of the tube and 'wb' drift created by shear and bending deformations of the individual tube members. Both of these values may vary considerably, depending on the properties of the tube. In order to force all columns of the 'flanges' or windward or leeward sides of a tube, to participate in resisting overturning moments by direct forces in columns, the sides of the tube must be sufficiently stiff to reduce what is known as 'shear lag'.

The tube concept of tubular system has numerous significant advantages over the other framing systems not only for reasons of economy and efficiency, but also for structural reasons, such as:

1. Because the wind resisting system is located on the perimeter of a building, maximum advantage is taken of the total width of the building to resist overturning moments.
2. Since the wind resisting system is concentrated on the perimeter it is generally possible to design the interior framing for gravity loads only. As a result, there is a greater freedom in locating columns and beams within the core, and their size is considerably reduced. Consequently, the core framing may be arranged to best suit the many non-structural requirements within the core, which in turn leads to a significant gain in rentable space.

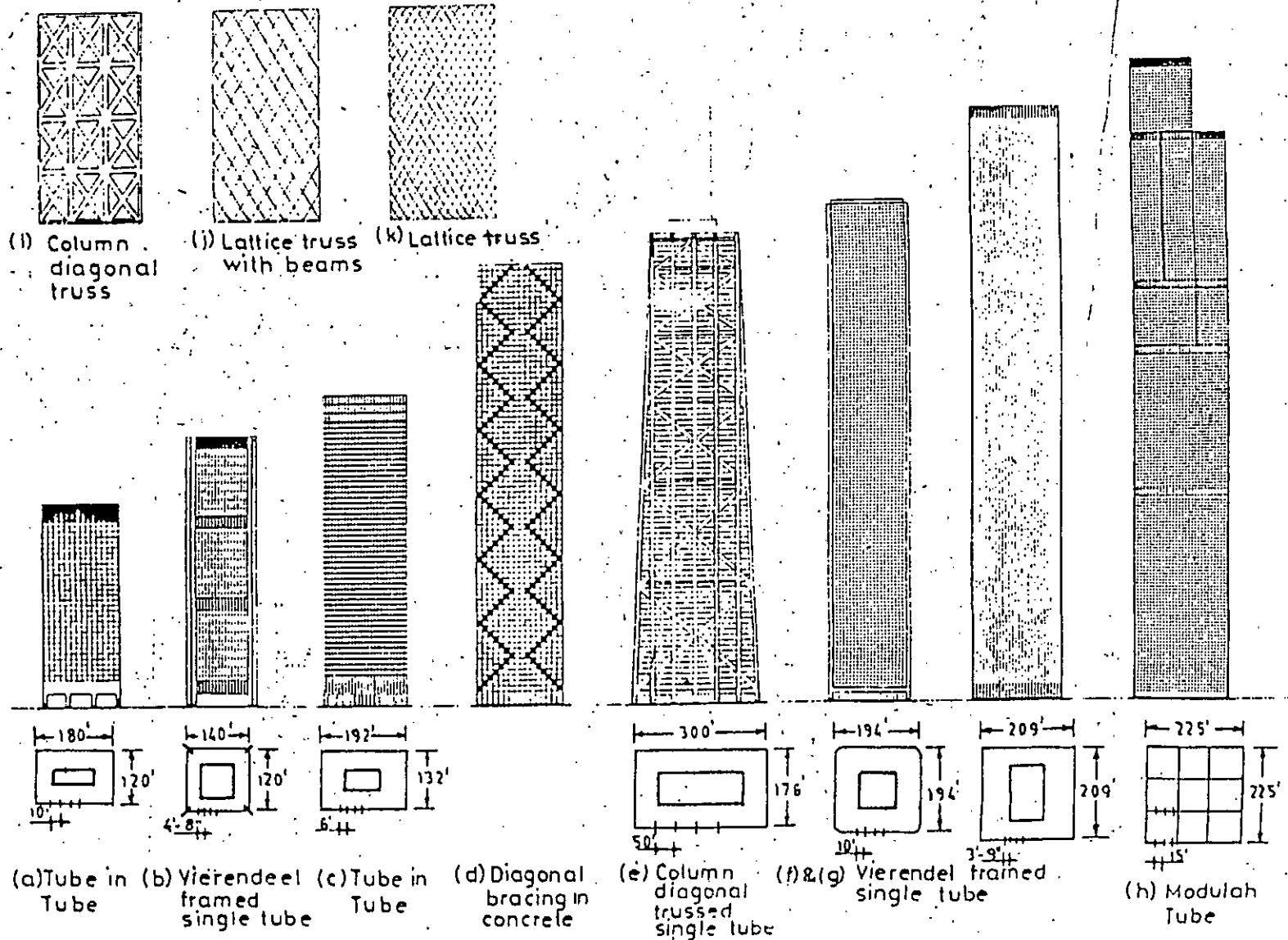


Fig. 1.1 Tubular Building Structures

3. The tube system leads to an identical framing for all floors, because the floor members are not subjected to varying internal forces due to lateral loads.

4. The tube concept also lead to a great number of identical framing units in the tube itself, which can be produced with standard forms allowing a very speedy erection. Frequently this advantage more than outweighs the fact that more elements must be constructed due to closer spacing the columns.

From the practical point of view there is another significant advantage; once the basic perimeter spandrel conditions have been resolved with the architects, the final analysis and design of the tube can proceed unaffected by the lengthy process of resolving detail layout and service requirement in the core area.

The tubular structures may be subdivided into the following types as shown in table 1.1

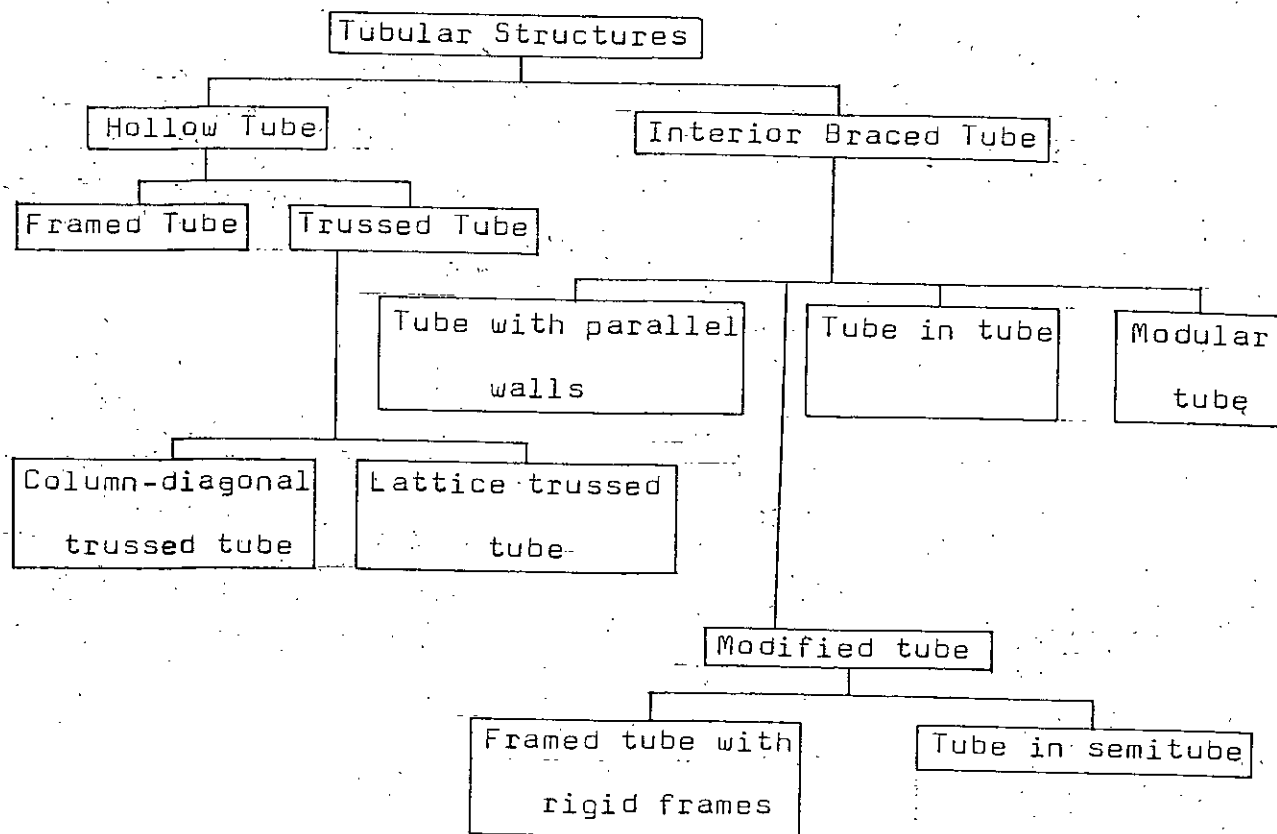
1.3.1 Hollow Tube

a) Framed Tube

The framed tube, the earliest application of the tubular concept was first used in the 43 storey Dewitt Chestnut Apartment Building in Chicago. In this Vierendeel tube system the exterior walls of the building, consisting of a closely spaced rectangular grid of beams and columns rigidly connected together resist lateral loads through cantilever tube action without using interior bracing. The interior columns are- assumed to carry

Table 1.1 Classification of tubular structures

(adopted from ref. 17)



gravity loads only and contribute very little to the lateral stiffness of the building (Fig. 1.2). The stiff floor act as diaphragms with respect to distributing the lateral forces to the perimeter walls.

Other examples of hollow framed tube buildings are the 83 storey Standard Oil Building in Chicago and 110 storey World Trade Center in New York (Fig. 1.1g). Although these buildings have interior cores they act as hollow tubes because the cores are not designed to carry lateral loads.

It would be ideal in the design of framed tube systems if the exterior walls were to act as a unit, responding to lateral

loads in pure cantilever bending. If this were the case all columns that makes up the tube, analogous to the fibres of a beam, would be either in direct axial tension or compression. The linear stress distribution that would result is indicated by broken lines in Fig. 1.5

However the tube behavior of the tube lies somewhere between that of a pure cantilever and a pure frame. The sides of the tube parallel to wind tend to act as independent multi-bay rigid frames given the flexibility results in wracking of the frame due to shear, called shear lag. Hence bending takes place in columns and beams.

The effect of shear lag on the tube action results in non-linear stress distribution along the column envelop; the columns at the corners of the building are forced to take a higher share of the load than the columns in between (Fig.1.5). Furthermore the total deflection of building no longer resemble a cantilever beam as shear mode deformation becomes more significant.

The shear problem severely affects the efficiency of the tubular system and all later developments of tubular design attempt to overcome it. The framed tube principle seems to be economical for steel buildings upto 80 stories and for concrete buildings upto 60 stories⁽¹⁷⁾.

b) Trussed Tube

The inherent weakness of the framed tube lies in the flexibility of its spandrel beams. Its rigidity is greatly improved by adding diagonal members. The shear is now primarily

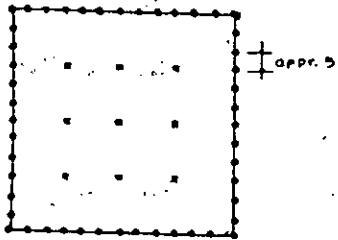


Fig. 1.2 Framed hollow tube

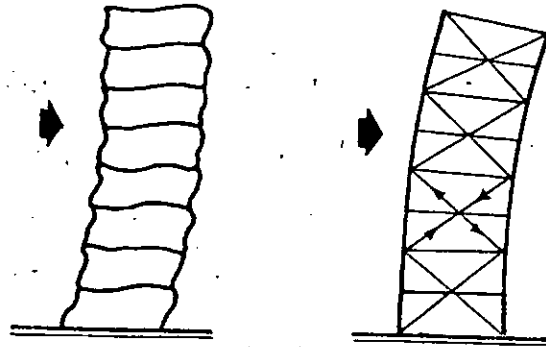


Fig. 1.3 Column-Diagonal Trussed Tube

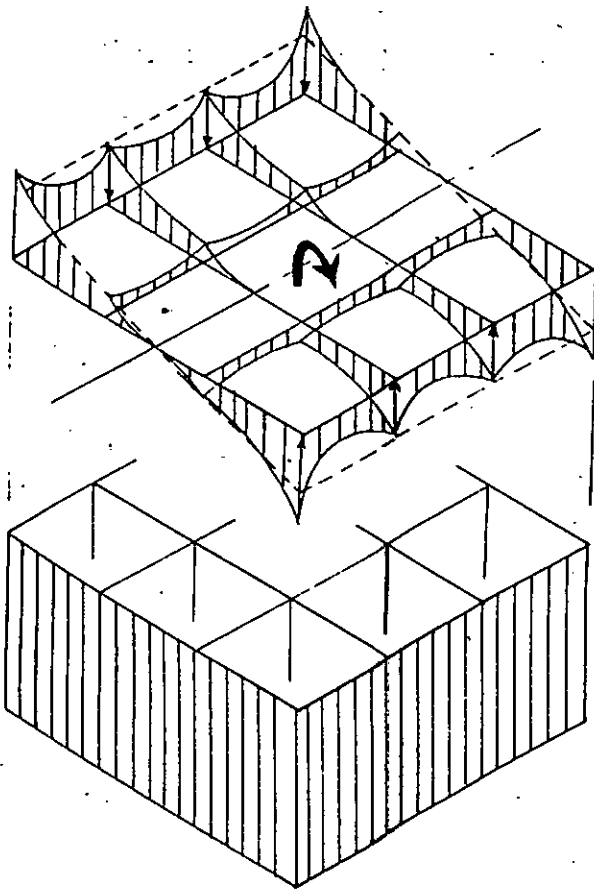


Fig. 1.4

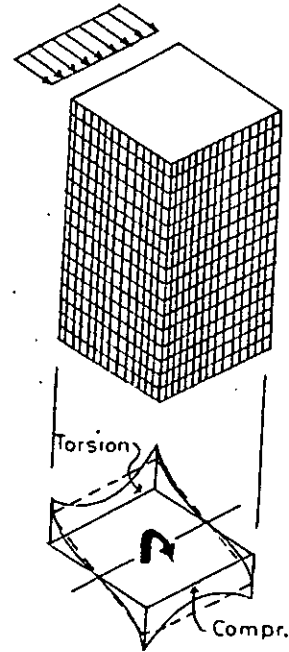


Fig. 1.5

absorbed by the diagonals, not by spandrels. The diagonals carry the lateral forces directly in the predominantly axial action. This reduction of shear lag provides for nearly pure cantilever behavior (Fig. 1.3)

b)(i) Column-diagonal Trussed Tube

This system uses diagonals within the rectangular grid of beams and columns (Fig. 1.1e). The diagonals together with the spandrel beams create a wall-like rigidity against lateral loads. Not only do the diagonals carry the major portion of wind loads they act as an inclined columns supporting gravity loads as well.

Normally the compression induced by gravity loads is not overcome by the tension caused by lateral loads. This dual function of the diagonal members make this system rather efficient for very tall building (upto about 100 stories in steel). This allows much larger spacing of columns than the framed tube.

b)(ii) Lattice Trussed Tube

In this system the tube is made up of closely spaced diagonals with no vertical columns (Fig. 1.1j,k). The diagonals act as inclined columns, carry all gravity loads and stiffen the structure against wind. The diagonals may be tied together by horizontal beams.

The diagonals are extremely efficient in responding to lateral loads but they are less efficient than vertical columns in transmitting the gravity loads to the ground. Furthermore, the large number of joints required between diagonals and the problems related to window details makes the lattice tube truss system generally impractical.

1.3.2 Interior Braced Tube

The framed exterior tube may be stiffened in plane by adding diagonals or it may be stiffened from within the building by adding shear walls or interior bracing are discussed in the following sections:

a) Tube with Parallel Shear Walls

The exterior tubular wall can be stiffened by incorporating interior shear walls in the plan. One can visualize the exterior tube wall as the flanges of a huge built-up beam system in which the shear walls represent the webs. The stresses in the exterior tube walls are primarily axial, since shear lag is minimised.

The example in Figs. 1.6(a) and 1.6(b) respectively, illustrate two approaches: wide spacing of facade columns, requiring a shear wall for every column and close spacing of facade columns requiring only two shear walls.

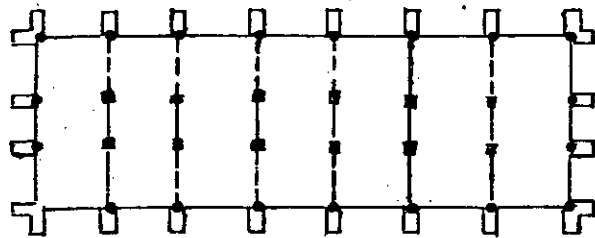


Fig. 1.6(a)

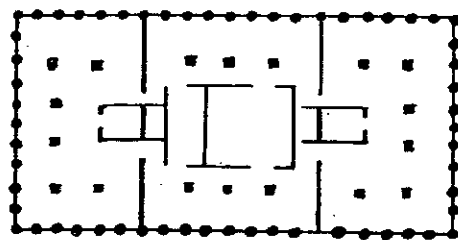


Fig. 1.6 (b)

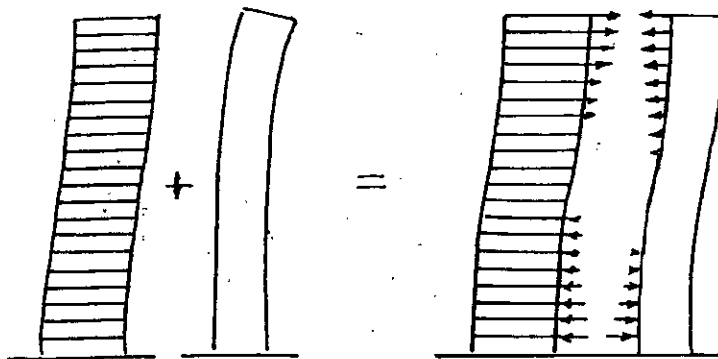


Fig. 1.7

b) Tube-in-Tube

The stiffness of a hollow tube system is very much improved by using the core not only for gravity loads but also to resist lateral loads as well. The floor structures tie the exterior and interior tubes together and they respond as a unit to lateral forces.

The reaction of a tube-in-tube system to wind is similar to that of a frame and shear wall structure. However the framed exterior tube is much stiffer than rigid frame.

Figure 1.7 indicates that the exterior tube resists most of the wind in the upper portion of the building, whereas the core carries most of the loads in the lower portion.

The tube in tube approach has been used in the 38 storey Brunswick Building in Chicago (Fig. 1.1c) and the 52 storey one shell Plaza Building in Houston (Fig.

Taking the tube in tube concept one step further, the designers of a 60 storey office building in Tokyo (Fig. 1.8) used a triple tube. In this system the exterior tube alone resists wind loads, but all three tubes, connected by floor systems interact in resisting earthquake loads.

c) Modified Tube

Tubular action is most efficient in round and nearly square buildings. Buildings deviating from these forms present

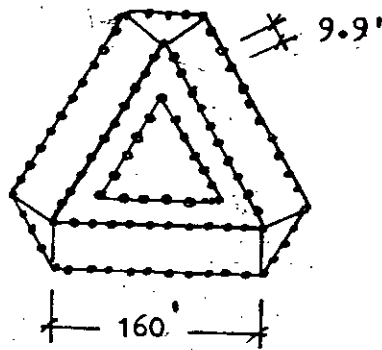


Fig. 1.8

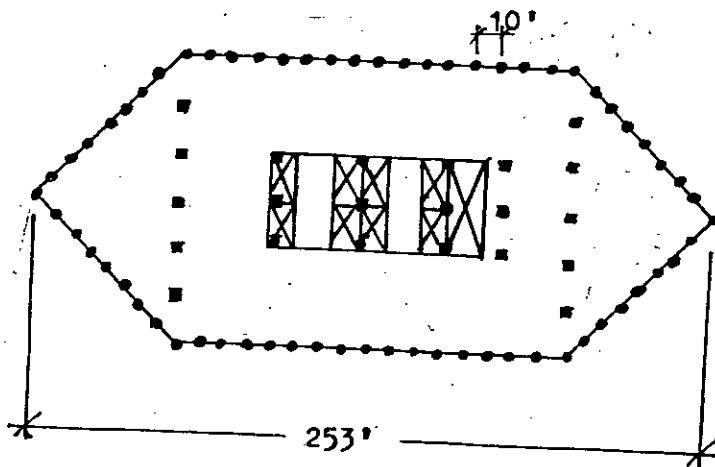


Fig. 1.9

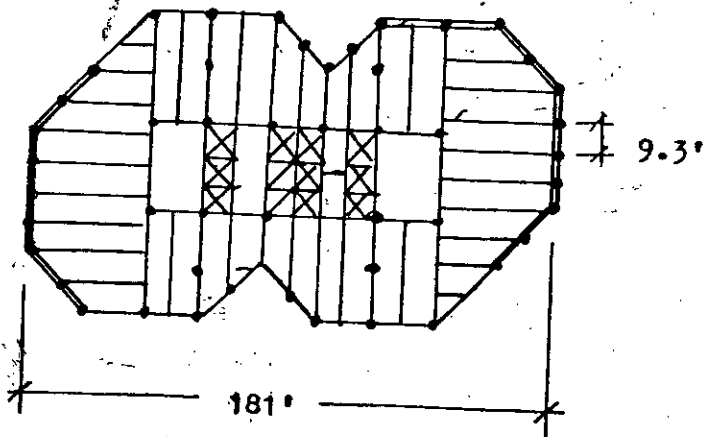


Fig. 1.10

special structural considerations when tubular action is desired. The following two examples describe such conditions.

i) Framed Tube-with Rigid Frames

The hexagonal shape of a 40 storey office building in Charlotte (Fig. 1.9) forced the designers to modify the tubular principle. The pointed ends of this hexagonal building exhibited excessive shear lag, making it impossible to get effective tubular response. Adding rigid frames in the transverse direction served to tie the exterior walls together. Thus the end of the triangular action was achieved.

ii) Tube in Semitube

The irregular plan of 32 storey Western Pennsylvania National Bank in Pittsburgh Fig. 1.10 give rise to still another special solution of tubular effect is generated by the exterior walls. In this building, however, the two intersecting octagons form a structural tube in the central part of the building.

The two end portions of the building are stiffened by channel like wall frame system. The wind is resisted by the combination of interior tube and the huge exterior end wall channels.

d) Modular Tubes

This latest development in tubular design is the modular or bundled tube principle. This system has been used for the

Shear's Building in Chicago, currently the tallest building of the world.

The exterior framed tube is stiffened by interior cross diaphragms in both directions (Fig. 1.4); an assemblage of cell tubes is formed. These individual tubes are independently strong, therefore, may be bundled in any configuration and discontinued at any level. A further advantage of this bundled tube system lies in extremely large floor areas that may be enclosed.

The interior diaphragms act as webs of a huge cantilever beam in resisting shear forces, this minimising shear lag. In addition, they contribute strength against bending.

The behavior of this system is shown in the stress distribution diagram in Fig. 1.4. The diaphragms parallel to wind (i.e. web) absorb shear, thereby generating points of peak stress at points of intersection with perpendicular walls (i.e. flanges) indicating the individual action on each tube.

1.4 Objective of the Thesis

- a) To develop a method to carry out preliminary analysis of non-rectangular tubular structure e.g. hexagonal shape.
- b) To develop a computer program based on this method.
- c) To check the accuracy of the method by comparing the results with those obtained from an 'exact' method of solution viz. space frame analysis.

- d) To study the shear-lag effect on tubular structures with different stiffness factors.

The study would be limited to the structures having one axis of symmetry and do not undergo significant torsion.

CHAPTER 2

REVIEW OF AVAILABLE APPROXIMATE METHODS OF ANALYSIS OF TUBULAR STRUCTURES

2.1 Introduction

The approximate methods of structural analysis are developed to enable the engineer to reach quick decisions regarding the dimensions and layout of structural members and to compare different schemes of structural systems. Although the availability of powerful and sophisticated computers encourage the engineers to go for exact analysis of the structures, the final design is often accomplished by shuttling between 'analysis' and 'design'; the starting (i.e. the preliminary design) and acceptance of the final design still require engineering judgement. In both cases, the engineers need to make short and hand calculations either to prepare 'analysis' or to assure himself that the 'computer results are at least realistic'.

2.2 Research on Shear-lag Analysis of Box Beams

Shear lag phenomenon, resulting in a non-uniform distribution of bending stresses across wide flanges of a beam cross-section has long been recognized. The analysis and design of box-beams with this special problem have also been investigated by aeronautical engineers. The pre-and-post-World War II periods are especially marked for researches on box-like components of

aircraft structure and so most of the significant papers on box-beams were published during this time.

A.H. Khan⁽¹³⁾ has extensively studied the past research on shear-lag analysis of box beams. Many early work on shear-lag problems are referred to in this thesis. He used energy theorems and calculus of variation to present a general solution for bending and twisting of thin walled closed tubular structure. He assumed the spanwise displacements of a beam in the form of finite series incorporating the chordwise (transverse) displacements as some chosen and simple functions. A number of simultaneous differential equations are obtained which can be solved for stress and displacements.

D.A. Foutch and P.C. Chang⁽¹¹⁾ have reported an interesting phenomenon associated with shear-lag in the flanges of box girders that is quite contrary to well established ideas concerning this subject. If a cantilever tube is loaded laterally under non-uniform shear, a reversal of the shear lag distribution may occur at some point in the beam; the center line stress may exceed the edge stress.

2.3 Works on Rigid-Tube Structures

Considering the number of buildings constructed all over the world using the rigid-tube concept, the published informations concerning their behavior under load is contained in a relatively few papers. The approximate method of analysis for

their preliminary design suggested by ACI Committee is probably among the first of the simplified methods of analysis. In this method, two distinct types of behavior of a framed tube structure are recognized, viz. the frame behavior of two sides parallel to wind direction, and the tube behavior of the entire structure. For the first action, the committee suggested the portal method of analysis of two parallel frames. For the second, the whole structure is simulated by vertical cantilevered beam with two discrete channels. To account for shear-lag effect, the effective flange width is taken as a function of the three external dimension of the tube⁽²⁾.

Coull and Bose⁽³⁾ method of analysis for framed-tube structure provides a simple closed form solution by replacing the discrete structure by an equivalent orthotropic tube and making simplifying assumptions regarding the stress distribution in the structure.

Coull and Subedi's^(4,5) method of analysis for framed tube structures is based on a modified plane frame computer program. By recognizing that the major interaction between the frames parallel and perpendicular to the lateral loads are vertical shear forces at the corners, the two orthogonal frames are considered to lie in the same plane and are connected in series by fictitious linking members whose stiffnesses are chosen to allow only vertical forces to be transmitted between frames. By recognizing this dominant mode of behavior, it is possible to reduce the analysis to that of an equivalent

plane frame, with a consequent large reduction in the amount of computation required in a conventional three dimensional analysis.

A simplified method is also presented by Ast and Schwighefer⁽¹⁾ for the analysis of framed-tube structures when subjected to bending due to lateral loading. The method consists in replacing the three dimensional tube by an equivalent two dimensional system. Several additional simplifications are assumed and their influence on the accuracy of the results is demonstrated.

An approximate method is also available from Chan, Tso and Heidebrecht⁽¹⁰⁾ to study the interacting effect of normal frames on uniform shear walls and the shear lag effect in the normal frames. Based on the axial deformation distribution among column, a reasonable assumptions is introduced to simplify the method.

Rigorous treatment of the analysis of a framed-tube structure has been presented by F.R. Khan and Amin⁽¹⁴⁾ and A.H. Khan⁽¹³⁾. F.R. Khan and Amin⁽¹⁴⁾ presented a graphical analytical solution for framed tubes of any dimension and of any height. Influence curves are presented for an equivalent 10-story tube with various ratios of bending stiffness of columns to shearing stiffness of beams, and different aspect ratios of the building. From these curves, the axial forces in the columns and shear forces in the spandrel beams of a

tube of any height can be obtained using a reduction modelling technique. A large number of computer runs on a 10-story equivalent plane frame were made to construct the influence curves for various factors. The effect of shear lag is taken into account by the nature of the computer analysis.

A.H. Khan suggested⁽¹³⁾ a simplified method of analysis of tube structures, which takes into account the effect of shear-lag in tube formed by uniform plates perforated by a large number of regular openings. The effect of rigid joint is also considered in constructing the mathematical model. The range of the method is then extended to include various tubular structures of different beam-column stiffness ratio, thickness and material variations in adjacent or opposite walls. He considered the framed tube as an equivalent solid thin walled beam. This method is limited to structures having height to width ratio greater than two and with relatively deep members. Also the properties of the structure must be constant across its width and along its height. The accuracy of the method is lost appreciably when the ratios of beam depth to story height and column depth to bay width are less than 0.25⁽¹⁶⁾.

A simplified method for the analysis of large multistory multibay framework has been presented by Kinn, Faul and Osama⁽¹⁶⁾. It is based on replacing the actual structure by an elastically equivalent orthotropic membername, which is then analysed by the finite element technique. The inflection

points for the bottom storey columns are assumed at $2/3$ of the story height from the base. The refined expressions for the equivalent elastic properties in combination with the versatility of the finite element technique make this method well adapted to wide range of tubular structure.

CHAPTER 3

SIMPLIFIED ANALYSIS OF TUBULAR STRUCTURE OF NON-RECTANGULAR SHAPE BY CONTINUOUS MEDIUM METHOD

3.1 Introduction

A simplified method of solution for high-rise tubular structures is presented in this chapter. This method is used to analyse the tubular structure of non-rectangular shape viz. hexagonal, octagonal etc. in plan. The continuous medium method proposed earlier by Choudhury⁽⁷⁾ for plane shear walls with multiple bands of openings has been extended by Bari⁽¹⁸⁾ to analyse the tubular structure of rectangular in plan. The method presented is the modification of Bari's⁽¹⁸⁾ method to analyse the structures of non-rectangular shape. The continuous medium method consists in replacing the spandrel beams by a continuous medium (Fig. 3.1), obtaining a series of ordinary differential equations for the shear forces in the continuous medium by minimising the strain energy and solving the equations by using a weighted residual method suggested by Galerkin. The main advantage of the method is that the solution time is independent of the number of stories and depends only on the number of columns. This makes it possible to contain approximate solutions for very rapidly using a small computer.

3.2 Assumptions

i) The connecting beams do not deform axially and hence the lateral deflection of individual walls is the same at any level.

ii) The moment of inertia and cross-sectional areas of the walls and the connecting beams are constant throughout the height, except the connecting beam at the topmost storey which has half the moment of inertia and half the cross-sectional area of the other beams.

iii) The point of contraflexure of the connecting beams at their mid span.

iv) Plane section of the wall before bending remains plane after bending, so that the moment curvature relations based on the simple engineers theory of bending (ETB) may be used.

From the assumptions (i) to (iv), it follows that the moment in the walls will be proportional to their stiffnesses. The proof of this is presented in Appendix-A.

3.3 General Formulation

The formulation technique has been adopted from Ph.D. thesis of Choudhury⁽⁷⁾. Fig. 3.3 shows a typical floor plan of a tubular structure, consisting of closely spaced columns at arbitrary locations and connected by deep spandrel beams at floor levels. It is assumed that the cross section of the column is rectangular and doubly symmetric. The discrete connecting beams of stiffness EI are replaced by a continuous medium connecting the walls for full height and having same

bending stiffness as the beams they replace. The structure is released by introducing a cut along the line of contraflexure and the integral of distributed shear forces in the connecting medium,

$$T = \int_0^z q dz \quad (3.1)$$

is taken as the redundant function (Fig. 3.2)

The governing equation for the function T will be derived from energy considerations (as originally suggested by Rosman). Neglecting the effect of axial forces the strain energy due to bending of the continuous medium of height dz is

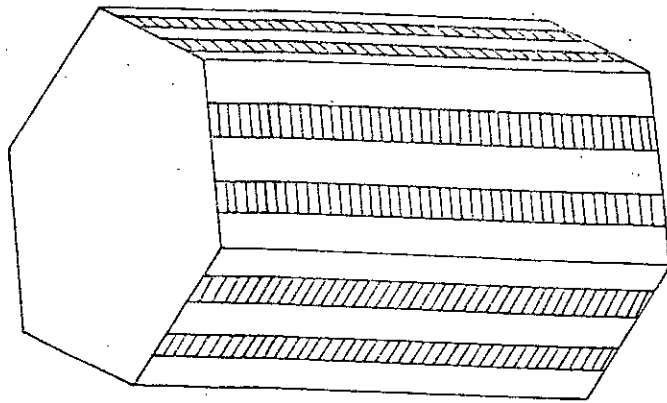
$$\delta U_{1,i} = 2 \left[\int_0^{\frac{b_i}{2}} \frac{(q_i x)^2 \cdot dx \cdot h_i}{2I_{p,i} E} + \frac{1.2 q_i^2 \cdot h_i \cdot dx}{2A_{p,i} G} \right] dz \quad (3.2)$$

Substituting the value of $G = \frac{E}{2(1+\nu)}$

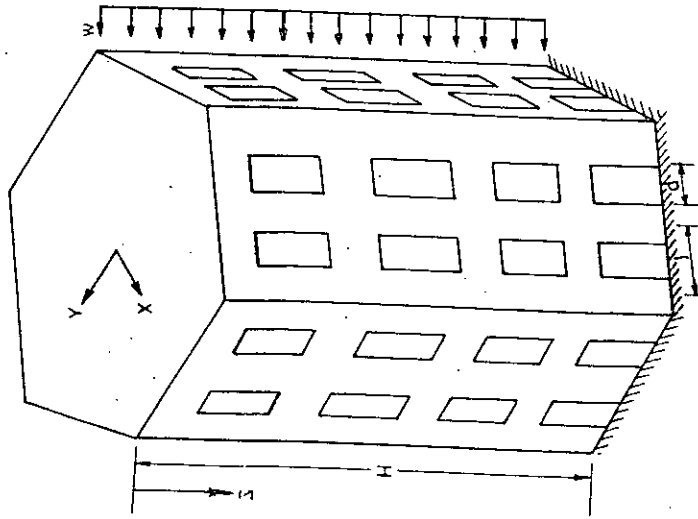
$$\text{Hence } \delta U_{1,i} = \frac{q_i^2 b_i^3 h_i}{24EI_{p,i}} \left[1 + 2.4 \left(\frac{d_i}{b_i} \right)^2 (1 + \nu) \right] dz \quad (3.3)$$

$$= (T_i)^2 \frac{b_i^3 h_i}{24EI_{c,i}} dz \quad (3.3)$$

$$\text{where } I_{c,i} = \frac{I_{p,i}}{1 + 2.4 \left(\frac{d_i}{b_i} \right)^2 (1 + \nu)} \quad \text{gives} \quad (3.4)$$



(a) Tube with openings



(b) Beams replaced by continuous medium

Fig. 3.1 Tube Structure.

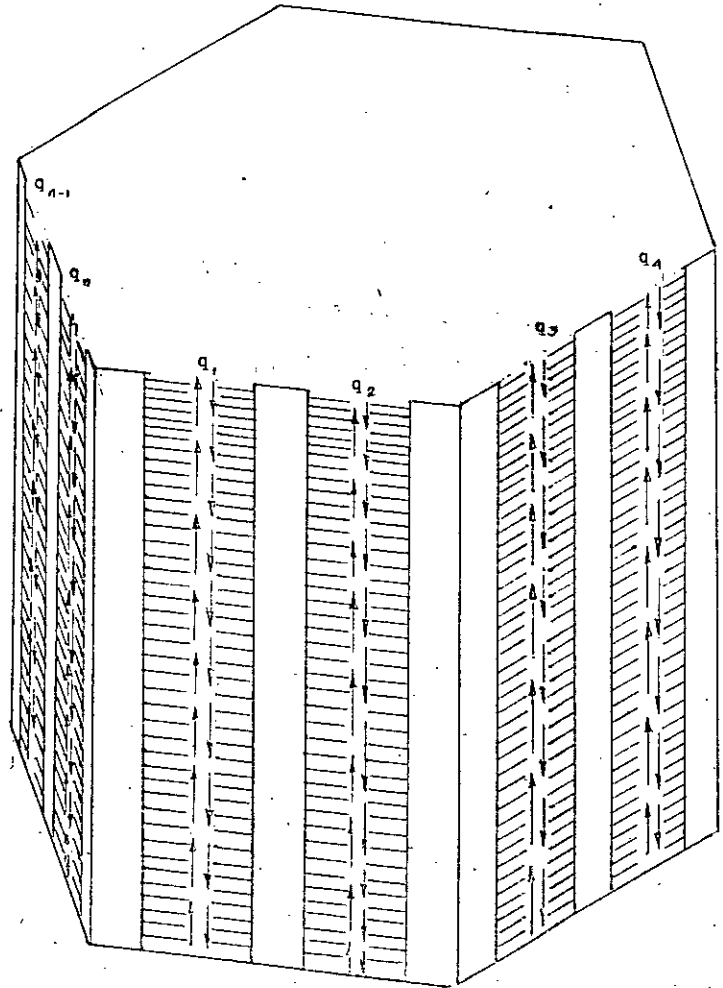


Fig. 3.2 Released structure

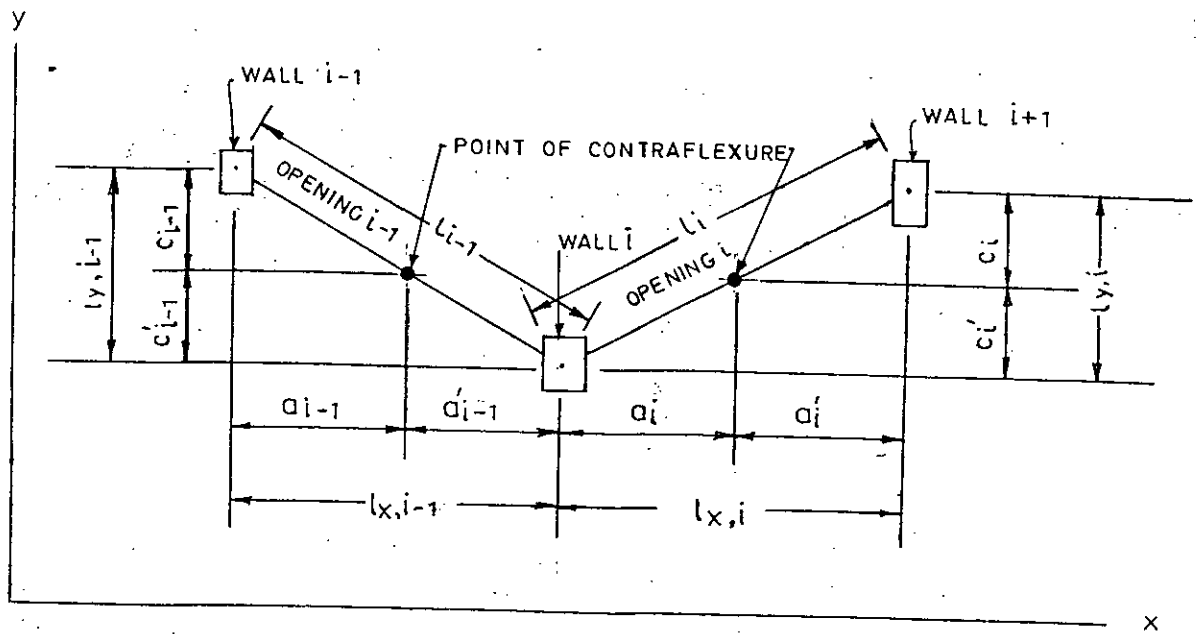
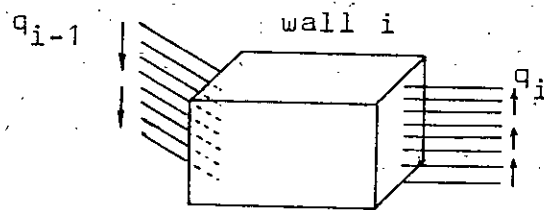
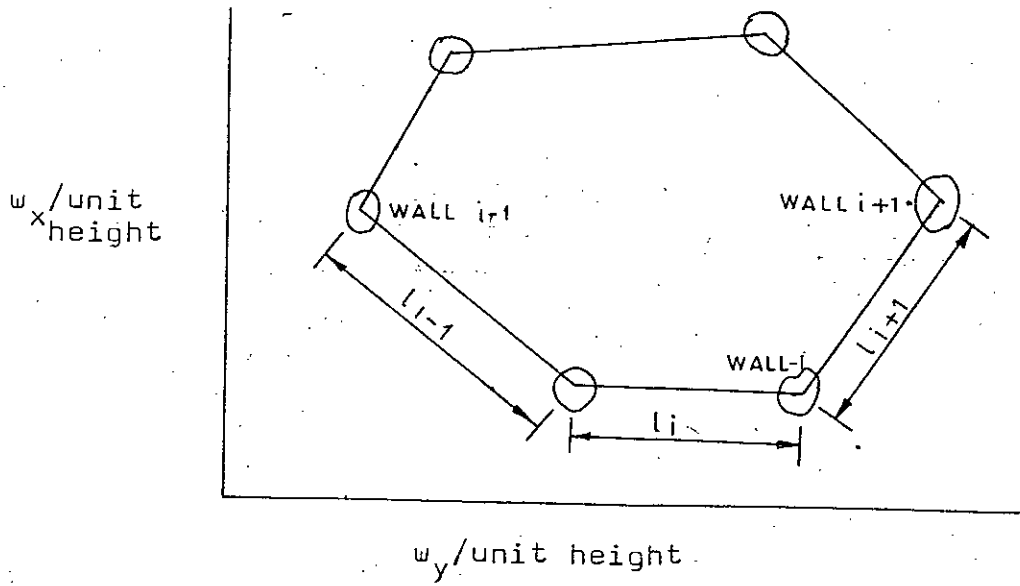


Fig. 3.3 Typical floor plan of a tubular structure.

The reduced moment of inertia-of the connecting beams with shear deformation induced.

Strain energy due to axial deformation in ith wall

$$U_{2,i} = \int_0^H \frac{(T_i - T_{i-1})^2}{2EA_i} dz \quad (3.5)$$

strain energy of ith wall due to bending deformation

$$U_{3,i} = \int_0^H \left[\frac{(M_{x,i})^2}{2EI_{x,i}} + \frac{(M_{y,i})^2}{2EI_{y,i}} \right] dz \quad (3.6)$$

As shown in Appendix-A the moments of walls is proportional to their stiffness, i.e., the total external moment will be distributed among the wall in proportion to the moment of inertia of the wall about global axis.

The bending moment $M_{x,i}$ and $M_{y,i}$ for any height z measuring from top of the tube, are expressed by

$$M_{x,i} = \frac{-\frac{w_y z^2}{2} + \sum_{j=1}^n (T_j C_j + T_{j-1} C'_{j-1})}{\sum_{j=1}^n I_{x,j}} I_{x,i} \quad (3.7)$$

$$M_{y,i} = \frac{\frac{w_x z^2}{2} - \sum_{j=1}^n (T_j a_j + T_{j-1} a'_{j-1})}{\sum_{j=1}^n I_{y,j}} I_{y,i} \quad (3.8)$$

For the tubular structures, due to continuity of the beams

$$T_0 = T_n \quad \text{and} \quad a'_0 = a'_n \quad (3.9)$$

$$\sum_{j=1}^n (T_j a_j + T_{j-1} a'_{j-1}) = (T_1 a_1 + T_0 a'_0) + (T_2 a_2 + T_1 a'_1) + \dots + (T_n a_n + T_{n-1} a'_{n-1}) \quad (3.10)$$

$$= \sum_{j=1}^n T_j l_{x,j} \quad (3.11)$$

Similarly $\sum_{j=1}^n (T_j c_j + T_{j-1} c'_{j-1}) = \sum_{j=1}^n T_j l_{y,j}$ (3.12)

putting the value of $M_{x,i}$ and $M_{y,i}$ in equation 3.6

we get

$$U_{3,i} = \int_0^H \left[\frac{\left\{ \frac{w_y z^2}{2} + \sum_{j=1}^n T_j l_{y,j} \right\}^2}{\sum_{j=1}^n I_{x,j}} \frac{I_{x,i}}{2EI_{x,i}} + \frac{\left\{ \frac{w_x z^2}{2} - \sum_{j=1}^n T_j l_{x,j} \right\}^2}{\sum_{j=1}^n I_{y,j}} \frac{I_{y,i}}{2EI_{y,i}} \right] dz$$

$$= \int_0^H \left[\frac{\left\{ \frac{-w_y z^2}{2} + \sum_{j=1}^n T_j l_{y,j} \right\}^2}{\sum_{j=1}^n I_{x,j}} \frac{I_{x,i}}{2E} + \frac{\left\{ \frac{w_x z^2}{2} - \sum_{j=1}^n T_j l_{x,j} \right\}^2}{\sum_{j=1}^n I_{y,j}} \frac{I_{y,i}}{2E} \right] dz$$

Now for all the walls the total strain energy due to bending is

$$U_3 = \int_0^L \left[\frac{\left\{ \frac{w_y z^2}{2} + \sum_{j=1}^n (T_j^1 y, j) \right\}}{\sum_{j=1}^n I_{x,j}} \right] \frac{I_{x,i}}{2E} + \left[\frac{\left\{ \frac{w_x z^2}{2} - \sum_{j=1}^n (T_j^1 x, j) \right\}}{\sum_{j=1}^n I_{y,j}} \right] \frac{I_{y,i}}{2E} dz \right]$$

$$= \int_0^L \left[\frac{\left\{ \frac{w_y z^2}{2} + \sum_{j=1}^n (T_j^1 y, j) \right\}}{2E \sum_{j=1}^n I_{x,j}} + \frac{\left\{ \frac{w_x z^2}{2} - \sum_{j=1}^n (T_j^1 x, j) \right\}}{2E \sum_{j=1}^n I_{y,j}} \right] dz \quad (3.13)$$

and

$$U_1 = \int_{i=1}^n \sum (T_i^1)^2 \frac{b_i^3 h_i}{24EI_{c,i}} dz$$

$$U_2 = \int_{i=1}^n \frac{(T_i - T_{i-1})^2}{2EA_i} dz$$

The total strain energy of the system

$$U = U_1 + U_2 + U_3 = \int F(Z, T, T') dz \quad (3.14)$$

The Euler equation of the calculus of variations states that if

$$\phi = \int F(Z, y, y') dz \text{ then for } \phi \text{ to be a minimum}$$

$$\frac{\partial F}{\partial y} - \frac{d}{dz} \left(\frac{\partial F}{\partial y'} \right) = 0 \quad (3.15)$$

Applying this to minimize the strain energy of the system, we will have

$$\frac{\partial U}{\partial T_i} - \frac{d}{dz} \left(\frac{\partial U}{\partial T_i'} \right) = 0 \quad (3.16)$$

$$\text{Now } \frac{\partial U}{\partial T_i} = \frac{\partial U_1}{\partial T_i} + \frac{\partial U_2}{\partial T_i} + \frac{\partial U_3}{\partial T_i} = 0 \quad (3.17)$$

$$\text{and } \frac{d}{dz} \left(\frac{\partial U}{\partial T_i'} \right) = \frac{d}{dz} \left(\frac{\partial U_1}{\partial T_i'} \right) + \frac{d}{dz} \left(\frac{\partial U_2}{\partial T_i'} \right) + \frac{d}{dz} \left(\frac{\partial U_3}{\partial T_i'} \right)$$

$$\frac{\partial U_1}{\partial T_i} = 0$$

$$\frac{\partial U_1}{\partial T_i} = \frac{T_i b_i^3 h_i}{12 E I_{c,i}} \quad (3.18)$$

$$\frac{d}{dz} \left(\frac{\partial U_1}{\partial T_i'} \right) = \frac{T_i'' b_i^3 h_i}{12 E I_{c,i}}$$

$$\text{Similarly } \frac{\partial U_2}{\partial T_i} = 0 \quad (3.19)$$

$$\frac{\partial U_2}{\partial T_i} = \frac{T_i - T_{i-1}}{A_i E} + \frac{(T_{i+1} - T_i)}{A_{i+1} E} \quad (-1)$$

and

$$\frac{\partial U_3}{\partial T_i} = \frac{-\frac{w_y z^2}{2} + \sum_{j=1}^n T_j l_{y,j}}{E \sum_{i=1}^n I_{x,i}} l_{y,j} + \frac{\frac{w_x z^2}{2} - \sum_{j=1}^n T_j l_{x,j}}{E \sum_{i=1}^n I_{y,i}} (-l_{x,i})$$

$$\frac{\partial U_3}{\partial T_i} = 0 \quad (3.20)$$

Substituting the above expressions in equation (3.16) yields

$$\frac{-\frac{w_y z^2}{2} l_{y,i}}{E \sum_{i=1}^n I_{x,i}} - \frac{\frac{w_x z^2}{2} l_{x,i}}{E \sum_{i=1}^n I_{y,i}} + \frac{\sum_{j=1}^n (T_j l_{y,j})}{E \sum_{i=1}^n I_{x,i}} l_{y,i} +$$

$$\frac{\sum_{j=1}^n (T_j l_{x,j})}{E \sum_{i=1}^n I_{y,i}} l_{x,i} - \left(\frac{T_{i+1} - T_i}{EA_{i+1}} \right) + \left(\frac{T_i - T_{i-1}}{EA_i} \right)$$

$$- \frac{T_i^3 b_i^3 h_i}{12EI_{c,i}} = 0 \quad (3.21)$$

Rearranging the terms,

$$T_i'' - \frac{12EI_{c,i}}{b_i^3 h_i} \left[\frac{\sum_{j=1}^n T_j l_{y,j}}{\sum_{i=1}^n I_{x,i}} l_{y,i} + \frac{\sum_{j=1}^n T_j l_{x,j}}{\sum_{i=1}^n I_{y,i}} l_{x,i} \right] + T_i \left(\frac{1}{A_i} + \frac{1}{A_{i+1}} \right) - \frac{T_{i-1}}{A_i} - \frac{T_{i+1}}{A_{i+1}} = 0$$

$$\left(\frac{w_x}{2} \frac{l_{x,i}}{\sum_{i=1}^n I_{y,i}} + \frac{w_y}{2} \frac{l_{y,i}}{\sum_{i=1}^n I_{x,i}} \right) \frac{12EI_{c,i}}{b_i^3 h_i} z^2 = 0$$

where $i = 1, 2, 3, \dots, n$ (3.22)

The above system of simultaneous second order differential equations may be written as

$$T_1'' - \alpha_{11}^2 T_1 - \alpha_{12}^2 T_2 \dots - \alpha_{1j}^2 T_j + \beta_1 z^2 = 0$$

$$T_2'' - \alpha_{22}^2 T_1 - \alpha_{22}^2 T_2 \dots - \alpha_{2j}^2 T_j + \beta_2 z^2 = 0$$

...

$$T_i'' - \alpha_{i1}^2 T_1 - \alpha_{i2}^2 T_2 \dots - \alpha_{ij}^2 T_j + \beta_i z^2 = 0 \quad (3.23)$$

where

$$\alpha_{ij}^2 = \left(\frac{l_{y,j} l_{y,i}}{\sum_{i=1}^n I_{x,i}} + \frac{l_{x,j} l_{x,i}}{\sum_{i=1}^n I_{y,i}} \right) \frac{12EI_{p,i}}{b_i^3 h_i} \quad \begin{matrix} \text{when } j \neq i \\ \neq i+1 \\ \neq i-1 \end{matrix}$$

$$\alpha_{ii}^2 = \left(\frac{l_{y,i}^2}{\sum_{i=1}^n I_{x,i}} + \frac{l_{x,i}^2}{\sum_{i=1}^n I_{y,i}} \right) \frac{12EI_{p,i}}{b_i^3 h_i}$$

$$\alpha_{i,i+1}^2 = \left(\frac{l_{y,i} l_{y,i+1}}{\sum_{i=1}^n I_{x,i}} + \frac{l_{x,i} l_{x,i+1}}{\sum_{i=1}^n I_{y,i}} - \frac{1}{A_{i+1}} \right) \frac{12I_{c,i}}{b_i^3 h_i}$$

$$\alpha_{i,i-1}^2 = \left(\frac{l_{y,i-1} l_{y,i}}{\sum_{i=1}^n I_{x,i}} + \frac{l_{x,i-1} l_{x,i}}{\sum_{i=1}^n I_{y,i}} - \frac{1}{A_i} \right) \frac{12I_{c,i}}{b_i^3 h_i}$$

$$\text{and } \beta_i = \frac{12I_{c,i}}{b_i^3 h_i} \left(\frac{w_x l_{x,i}}{2 \sum_{i=1}^n I_{y,i}} + \frac{w_y l_{y,i}}{2 \sum_{i=1}^n I_{x,i}} \right) \quad (3.24)$$

written in matrix notation, equation (3.21) becomes

$$\frac{d^2}{dz^2} \begin{bmatrix} T_1 \\ T_2 \\ \vdots \\ T_n \end{bmatrix} = \begin{bmatrix} \alpha_{11}^2 & \alpha_{12}^2 & \dots & \alpha_{1n}^2 \\ \alpha_{21}^2 & \alpha_{22}^2 & \dots & \alpha_{2n}^2 \\ \vdots & \vdots & \ddots & \vdots \\ \alpha_{n1}^2 & \alpha_{n2}^2 & \dots & \alpha_{nn}^2 \end{bmatrix} \begin{bmatrix} T_1 \\ T_2 \\ \vdots \\ T_n \end{bmatrix} + z^2 \begin{bmatrix} \beta_1 \\ \beta_2 \\ \vdots \\ \beta_n \end{bmatrix}$$

$$\text{or, } \frac{d^2}{dz^2} T = A.T. + \beta.z^2 \quad (3.25)$$

An analytical solution of the above system of equation is too tedious for more than two bands of openings.

The boundary conditions for the equations are:

$$\text{at } z = 0 \quad T_i = 0 \quad (i = 1, 2, 3, \dots, n)$$

$$\text{at } z = H, \quad \frac{dT_i}{dz} = 0 \quad (i=1, 2, 3, \dots, n) \quad (3.26)$$

Assuming a family of solutions

$$T_j = \sum_{i=1,3,5}^{\infty} a_{ij} \sin \frac{i\pi z}{2H} \quad (j = 1, 2, \dots, n) \quad (3.27)$$

each term of which satisfies the boundary conditions (eq. 3.26) and applying Galerkin's method to minimize the residuals, following system of simultaneous equations in the a_{ij} is obtained:

$$\begin{bmatrix} \frac{i^2 \pi^2}{4H^2} + \alpha_{11}^2 & \alpha_{12}^2 & \dots & \alpha_{1n}^2 \\ \alpha_{21}^2 & \frac{i^2 \pi^2}{4H^2} + \alpha_{22}^2 & \dots & \alpha_{2n}^2 \\ \alpha_{n1}^2 & \alpha_{n2}^2 & \dots & \frac{i^2 \pi^2}{4H^2} + \alpha_{nn}^2 \end{bmatrix} \begin{bmatrix} a_{i,1} \\ a_{i,2} \\ \dots \\ a_{i,n} \end{bmatrix} = \frac{16H^2}{3^3} (\pi_i \sin \frac{\pi i}{2})^{-2} \begin{bmatrix} \beta_1 \\ \beta_2 \\ \dots \\ \beta_n \end{bmatrix}$$

where $i = 1, 3, 5, \dots$

(3.28)

In matrix form

$$[C] [D_i] = [K]$$

the solution of which gives a_{ij} 's

$$[D_i] = [C]^{-1} [K] \quad (3.29)$$

Once the a_{ij} 's are determined, the values of the T 's at different heights may be evaluated by summing the series.

For wall i , at height z ,

$$M_{x,i} = \frac{-\frac{w_y z^2}{2} + \sum_{j=1}^n (R_j l_{x,j})}{\sum_{j=1}^n I_{x,j}} I_{x,j} \quad (3.30)$$

$$M_{y,i} = \frac{\frac{w_x z^2}{2} - \sum_{j=1}^n (T_j l_{x,i})}{\sum_{j=1}^n I_{z,j}} I_{y,i}$$

where T_j 's are calculated at height z .

Axial force in wall i at height z

$$F_i = T_i - T_{i-1} \quad (3.31)$$

Deflections:

Using moment curvature relationship

$$EI \frac{d^2 y_x}{dz^2} = \left(\frac{w_x z^2}{2} - \sum_{i=1}^n T_i l_{xi} \right)$$

$$EI \frac{d^2 y_y}{dz^2} = \left(\frac{w_y z^2}{2} - \sum_{i=1}^n T_i l_{yi} \right)$$

Substituting the values of T_i 's from equation 3.27

$$EI \frac{d^2 y_x}{dz^2} = \frac{w_x z^2}{2} - \sum_{j=1}^n \left(\sum_{i=1,3,5}^{\infty} a_{ij} \sin \frac{i\pi z}{2H} \right) l_{x,j}$$

$$EI \frac{d^2 y_y}{dz^2} = \frac{w_y z^2}{2} - \sum_{j=1}^n \left(\sum_{i=1,3,5}^{\infty} a_{i,j} \sin \frac{i\pi z}{2H} \right) l_{y,i} \quad (3.32)$$

Integrating twice, and substituting the appropriate boundary conditions,

$$\left(\text{at } z = H, y_x = y_y = \frac{dy_x}{dz} = \frac{dy_y}{dz} = 0\right)$$

$$\therefore EIy_x = \frac{w_x}{2} \left(\frac{z^4}{12} - \frac{H^3 z}{3} + \frac{H^4}{4} \right) - \frac{4H^2}{2} \sum_{j=1}^n \left[\sum_{i=1,3,5}^{\infty} a_{ij} \left(\frac{\sin \frac{i\pi}{2} - \sin \frac{i\pi z}{2H}}{i^2} \right) \right] l_{x,j}$$

and

$$EIy_y = \frac{w_y}{2} \left(\frac{z^4}{12} - \frac{H^3 z}{3} + \frac{H^4}{4} \right) - \frac{4H^2}{2} \sum_{j=1}^n \left[\sum_{i=1,3,5}^{\infty} a_{ij} \left(\frac{\sin \frac{i\pi}{2} - \sin \frac{i\pi z}{2H}}{i^2} \right) \right] l_{y,j} \quad (3.33)$$

For point Load at Top

The derivation follows exactly the same pattern as for the uniformly distributed load, the only difference is in values of loading terms in equation (3.25) expressed by $[B] z^2$, which is now replaced by

$$[B] z \quad \text{where } [B] = \begin{bmatrix} \beta_1 \\ \beta_2 \\ \beta_n \end{bmatrix} \quad \text{and} \quad \beta_i = \frac{12I_{ci}}{b_i h_i} \left(\frac{P_x l_{x,i}}{\sum I_{y,i}} - \frac{P_y l_{y,i}}{\sum I_{x,i}} \right) \quad (3.34)$$

where P_x and P_y are the concentrated load applied horizontally at top.

In equations (3.28) the K matrix

$$\text{becomes } \left[\frac{K}{-} \right] = \frac{8H}{i^2 \pi^2} \sin \frac{i\pi}{2} \begin{bmatrix} \beta_1 \\ \beta_2 \\ \beta_n \end{bmatrix} \quad (3.35)$$

The equation for moment (3.30) is modified to

$$M_{x,i} = (P_{y,z} - \sum_{i=1}^n T_i l_{y,i}) \frac{I_{x,i}}{\sum_{i=1}^n I_{x,i}}$$

$$M_{y,i} = (P_{x,z} - \sum_{i=1}^n T_i l_{x,i}) \frac{I_{y,i}}{\sum_{i=1}^n I_{y,i}} \quad (3.36)$$

and equation for deflection becomes

$$EI y_x = P_x \left(z^3/6 - \frac{H^2 z}{2} + \frac{H^3}{3} \right) - \frac{4H^2}{\pi^2} \sum_{j=1}^n \left[\sum_{u=1,3,5}^{\infty} a_{ij} \frac{\sin \frac{i}{2} - \sin \frac{i z}{2H}}{i^2} \right] l_{x,j}$$

$$EI y_y = P_y \left(\frac{z^2}{6} - \frac{H^2 z}{2} + \frac{H^3}{3} \right) - \frac{4H^2}{\pi^2} \sum_{j=1}^n \left[\sum_{i=1,3,5}^{\infty} a_{ij} \frac{\sin \frac{i\pi}{2} - \sin \frac{i\pi z}{2H}}{i^2} \right] l_{y,j} \quad (3.37)$$

3.4 Computer Program

A computer programme, based on the theory presented in section 3.2 and 3.3 has been written in FORTRAN. The sequence of operations followed in the programme is outlined in flow diagram presented in Appendix-C. The number of terms to be considered in series solution for the T's is read in as data.

The matrix formulation of the analysis automatically divides the programme into suitable sections. The A, B, C and K matrices have to be formed for each term of the series and the D_i's are obtained by solving equation (3.26)

$$\boxed{\underline{D}_i} = \boxed{\underline{C}^{-1}} \boxed{\underline{K}}$$

The size of the matrices to be handled, dependent only on the number of bands of openings, are usually small viz. (n x n) and do not present any storage-problems. A listing of the programme, together with a more detailed discussion of procedures and form of data input, is given in Appendix-C.

3.5 Modification for Non-rectangular Shape

In the method described in the section 3.2 and 3.3 the columns are considered rectangular and doubly symmetric. For rectangular shape of building the position of column is parallel to the global axes of the structure. Hence the moments of inertia of the column about their local principal axes are

the same for all the columns as the axes are parallel to global axes. But in non-rectangular building the local axes of the column are no longer parallel to the global axes because of their position in the structure. But as given in Appendix-A. The external moment is shared by the wall or column in proportion of the moment of inertia of the wall or column about global axes. Hence to use equation (3.7) and (3.8) the moment of inertia of the wall about the local axes should be transferred to the global axes. In Fig. (3.6) x-y are the global axes and u-v are local axes of the wall which makes an angle θ with global axes.

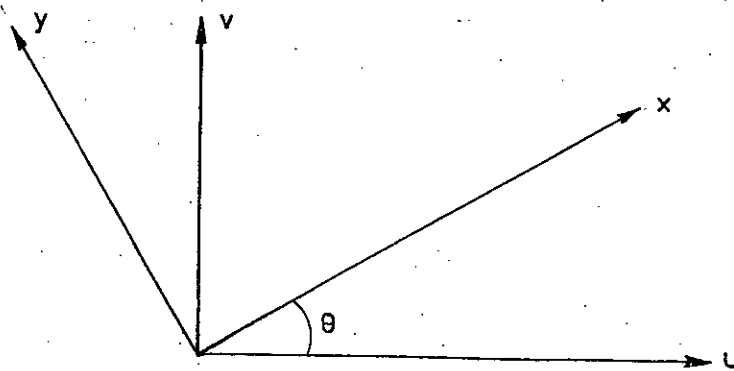


Fig. 3.6

The moment of inertia about x and y are I_x and I_y and similarly the moment of inertia about u and v axes are I_u and I_v . Hence

$$I_x = I_u \cos^2 \theta + I_v \sin^2 \theta$$

$$I_y = I_v \cos^2 \theta + I_u \sin^2 \theta \quad (3.38)$$

The moment of inertia of the walls used in eq. (3.7) and (3.8) are about global axes. Hence to get these global moment of inertias eq. (3.8) is used.

CHAPTER 4

RESULTS AND DISCUSSIONS

4.1 Introduction

In order to demonstrate the applicability of the method to tubular structures of non-rectangular plan shape, an example problem of a 20-storied building, hexagonal in plan, is analyzed for different stiffness parameters. The results of this example problem are presented in graphical and tabular forms. The axial forces in columns, shear forces in beams and lateral deflections of the buildings are calculated by the continuous medium method and the results obtained by this method are compared with those obtained from the more 'exact' space frame analysis. The effect of shear lag on this hexagonal shape of structure is also studied for different stiffness factors.

Fig. 4.1 shows the details of the 20-storey concrete rigid tube structure which was analyzed. The total height of the tube is 200 ft and it has 18 columns spaced 8 ft c/c, each side of the hexagon has a length of 24 ft. The other properties of the tube are

Storey height = 10.0 ft

Poisson's ratio = 0.18

Modulus of elasticity = 432,000 ksf

Two loading cases are considered, viz. (a) point load at the top and (b) uniformly distributed load. Three different 10-storey,

equivalent stiffness factors are considered for the same structure. The storey height and the center to center distance between the columns are kept fixed, only the beam size is changed to get the different stiffness factor. The stiffness factor can be defined as

$$S_f = \frac{S_b}{S_c}$$

where S_b = shear stiffness of spandrel beams

$$= \frac{12EI_b}{L^3}$$

and S_c = Axial stiffness of the column

$$= \frac{A_c E}{H}$$

where I_b = moment of inertia of the spandrel beams

A_c = area of cross section of the column

H = height of the column

L = effective span of the spandrel beam

E = modulus of elasticity

Actual stiffness factor of structure is transferred to a 10-storey equivalent stiffness factor S'_{f10}

$$\text{where } S'_{f10} = S_f \times \left(\frac{N}{10}\right)^2$$

where N = No. of storey.

The properties of the three tubes are given in Table 4.1 where the structures having three stiffness ratios (S'_{f10}) 0.1, 1.0 and 10.0 are considered. All these tubes are subjected to two types lateral loading (i) 90^k point load applied at the top and (ii) 30 psf UDL load.

4.2 Results Obtained by Continuous Medium Method

A hexagonal structure is analysed by the continuous medium method. The column axial forces are calculated by the continuous medium method for each tube under these two loading conditions. The variation of column axial force is shown on the Figs. 4.2 to 4.13 as a firm line.

The deflected shapes of the tube of different stiffness factor (S'_{f10}) are shown in Fig. 4.14 to 4.17 under different loading conditions.

4.3 Comparison between Continuous Medium Method and Space Frame Method

In order to check the accuracy of the continuous Medium method, all the tubes given in Table 4.1 are analysed by the space frame method. In this space frame method the beam and column elements are replaced by live elements and the rigidity due to the width and depth of beam/column is neglected. However this method gives the more exact result for the beams or columns of smaller dimension. The column axial forces calculated by the space frame method are compared with those

Table 4.1

Properties of the Tube

Beam width ft	Beam depth ft	Beam moment of inertia ft ⁴	c/c dis- tance between column ft	S_b/E ft	Column area ft ²	Storey height ft	S_c/E ft	S_f	No. of storey	S' f10
1.2	1.45	0.3048	8	0.007	2.88	10	0.288	0.025	20	0.1
1.2	3.132	3.072	8	0.072	2.88	10	0.288	0.25	20	1.0
2.0	5.69	30.703	8	0.72	2.88	10	0.288	0.5	20	10.0

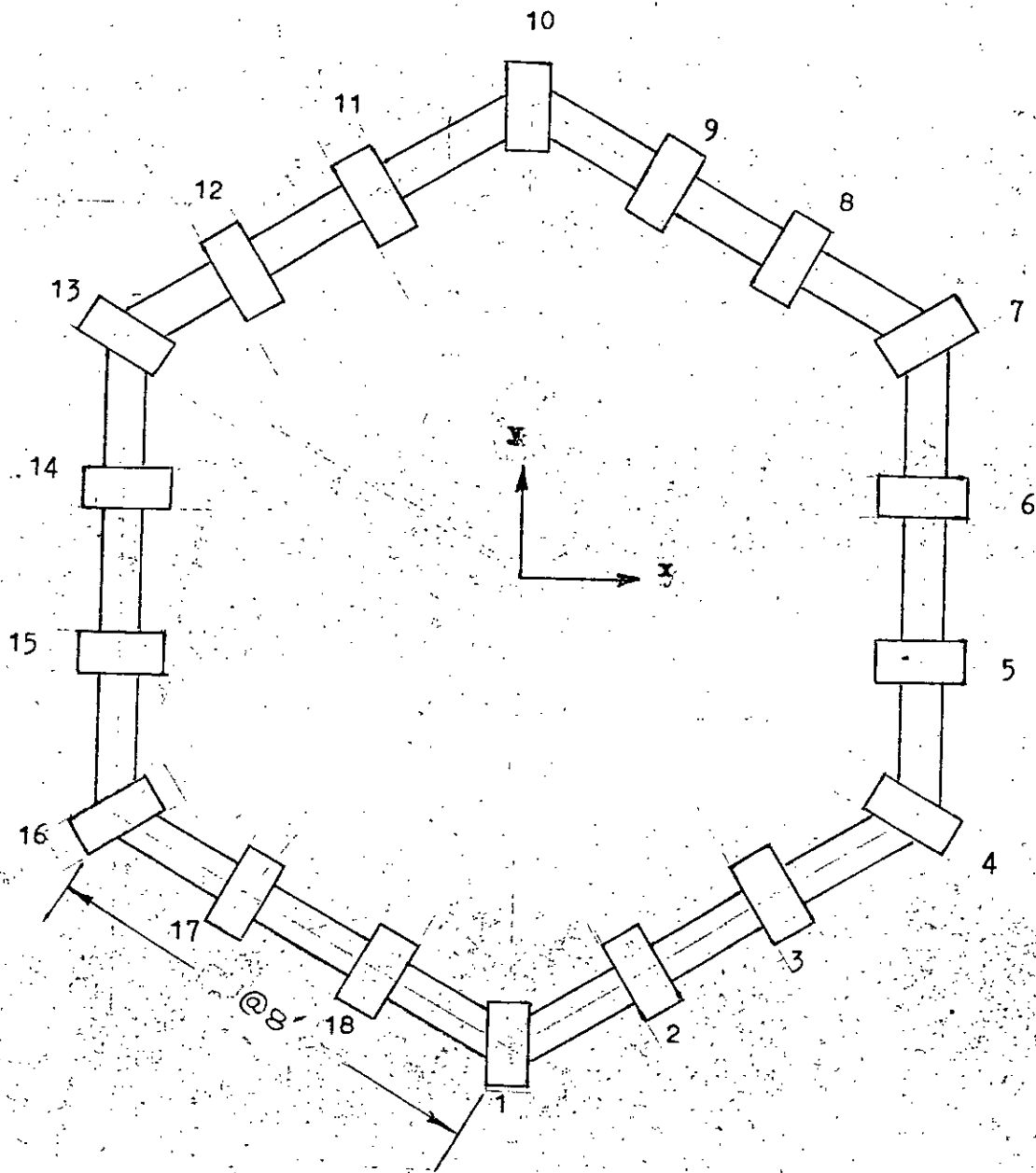


Fig. 4.1 Plan of the example problem

obtained from the continuous medium method and these are shown in Figs. 4.2 to 4.13. The variation of the column axial forces calculated by the 3-D space frame analysis are shown in Fig. 4.2 to 4.13 as dotted lines.

For a concentrated load 90^k applied at the top in x direction the results obtained by continuous medium method agree very well with those obtained by 3D space frame method upto level $Z/H = 0.75$ from top for $S'_{f10} = 1.0$ and 10.0 . But in case of $S'_{f10} = 0.1$ the values obtained by the space frame method are higher by 10% at level $Z/H = 0.75$ at the corner columns viz. column no. 4,7,13,16 and less by 8% at the columns in between viz. 3,8,12,17.

But at the base the difference between the results obtained by the two methods is higher; in the corner columns, viz. 4,7,13,16, the values obtained by space frame method are higher by 20% for $S'_{f10} = 10$, 23% for $S'_{f10} = 1$ and 14%, for $S'_{f10} = 0.1$ than those obtained by continuous medium method. On the other hand, for the columns in between, viz. column no. 3,8,12,17, the values are less by 14% for $S'_{f10} = 0.10$ 25% for $S'_{f10} = 1.0$, 26% for $S'_{f10} = 10.0$. For the load in the y direction similar types of results are obtained.

For a UDL of 30 psf applied in x direction, the results agree well at level $Z/H = 0.5$ and 0.75 , for all the stiffness factors. A reversal in the axial force distribution pattern is observed in both the methods upto level $Z/H = 0.5$, where

the axial loads carried by the corner columns are less than the adjacent columns as shown in Fig. 4.8 to 4.10.

As the case of point load, the column axial forces at the base, i.e. $Z/H = 1$, are higher in the corner columns than the adjacent one for UD loading both in the x and y directions. The values of column axial forces at corner columns 4, 7, 13, 16 obtained by the 3D space frame method is higher by 16.8% for $S'_{f10} = 0.1$, 33% for $S'_{f10} = 1$, and 31% for $S'_{f10} = 10$ for loading in x-direction than those values obtained by continuous medium method.

Similar types of variation is observed for the loading in y direction.

4.4 Discussion on Shear-lag Effect on Tubular Structure

The shear lag effect is also investigated on the tubular structures described earlier. It is observed that the shear lag effect is almost negligible for all the structures upto $Z/H = 0.5$ from tip. The pronounced affect on shear-lag on the stress distribution is observed at the base level for all the stiffness ratios under point load as well as uniformly distributed load.

It is observed that for uniformly distributed load from the top down to level $Z/H = 0.5$, the load carried by corner column is less than the adjacent columns and at lower level

i.e, from $Z/H = 0.5$ to the base the corner column takes the higher load than the adjacent columns. This may be due to the fact that the upper portion of the tube, the bending deformation is more prominent than the shear deformation. While in the lower levels of the tube, the shear deformation being more prominent than the bending deformation causes corner column to carry higher and axial load.

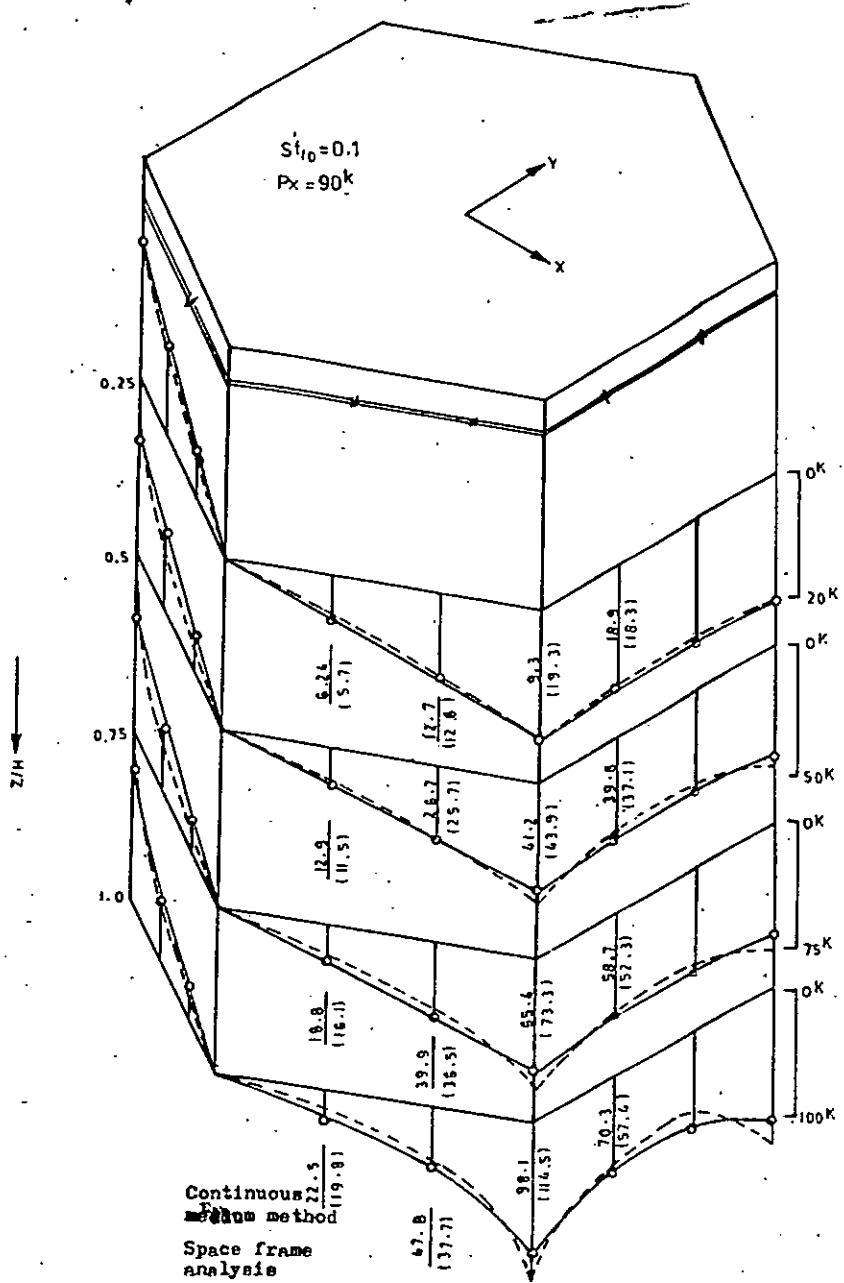


Fig.4.2 Shear-lag effect on hexagonal tubular structure
 (Values within parenthesis from space frame analysis)

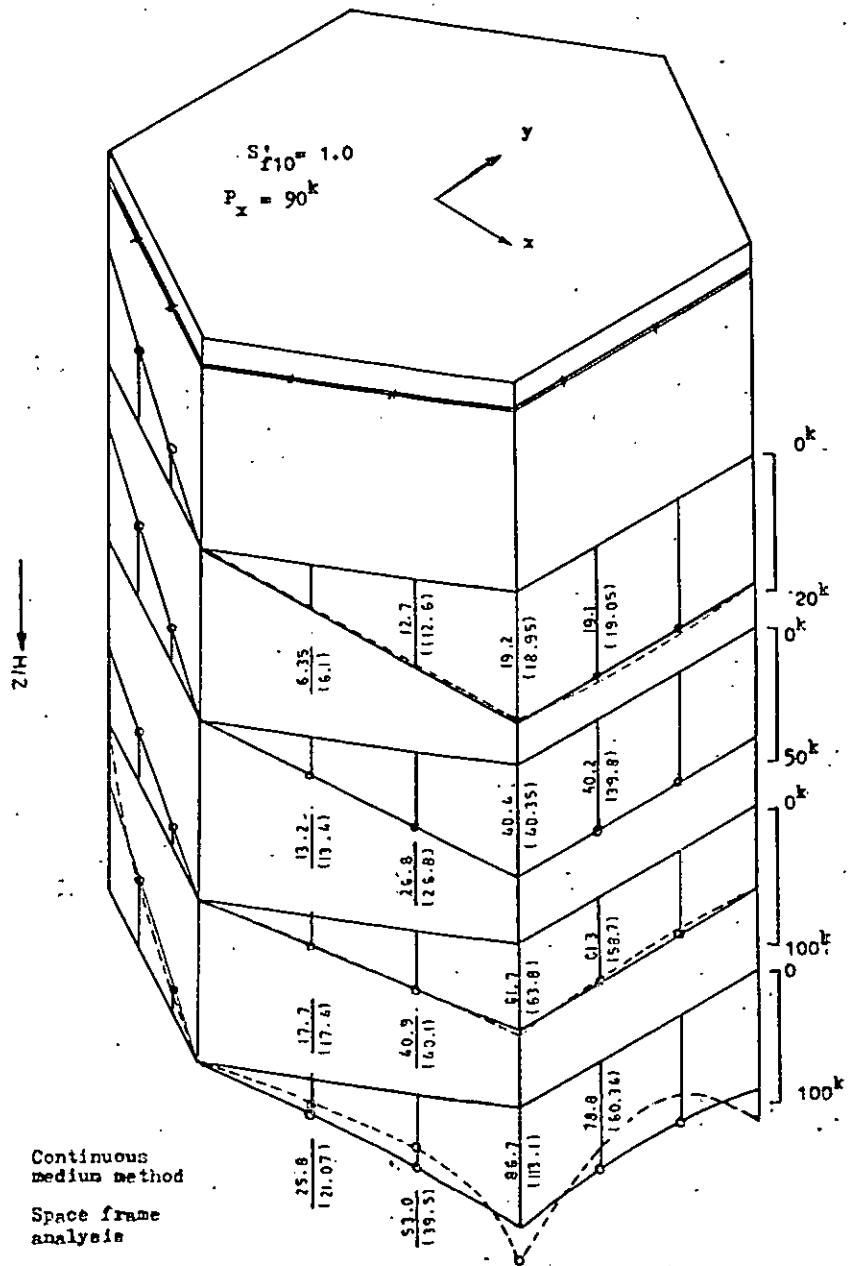


Fig. 4.3 Shear-lag effect on hexagonal tubular structure (values within parenthesis from space frame analysis)

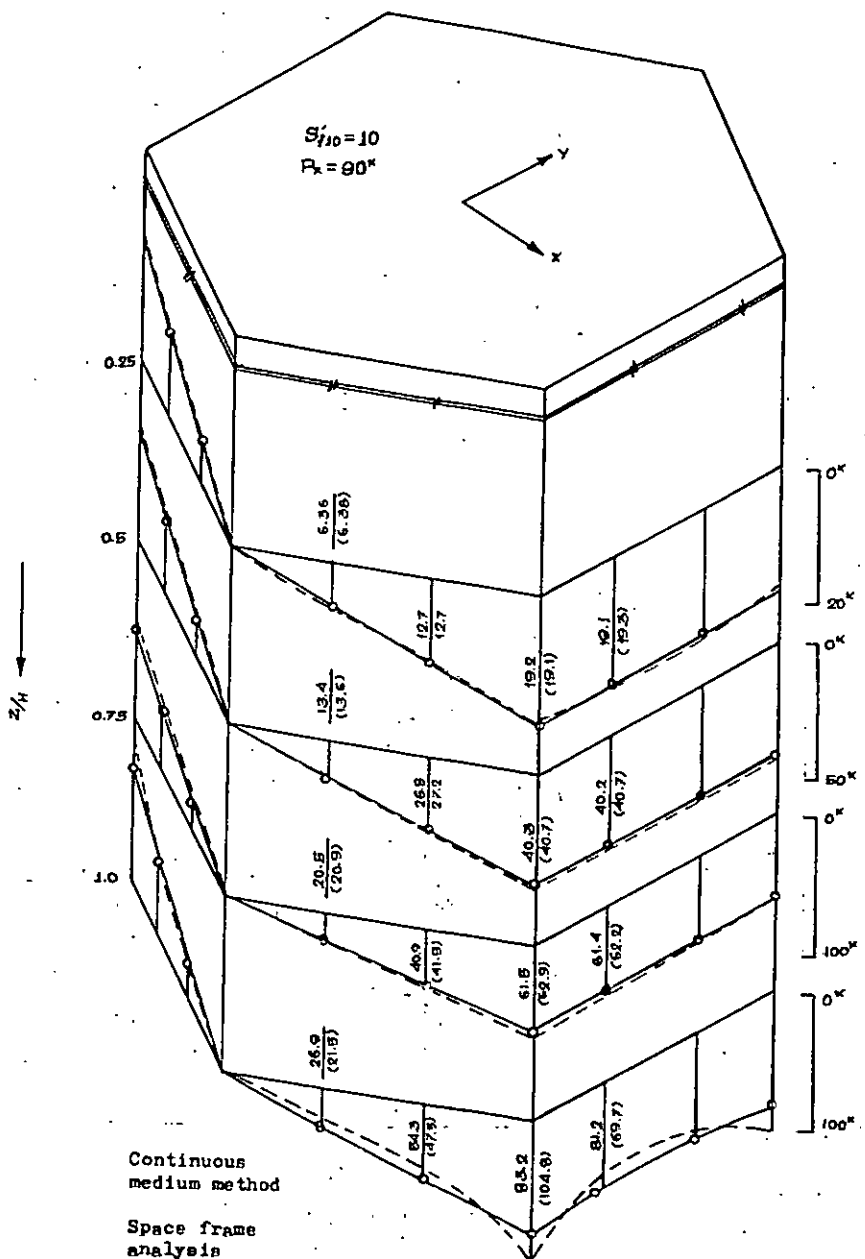
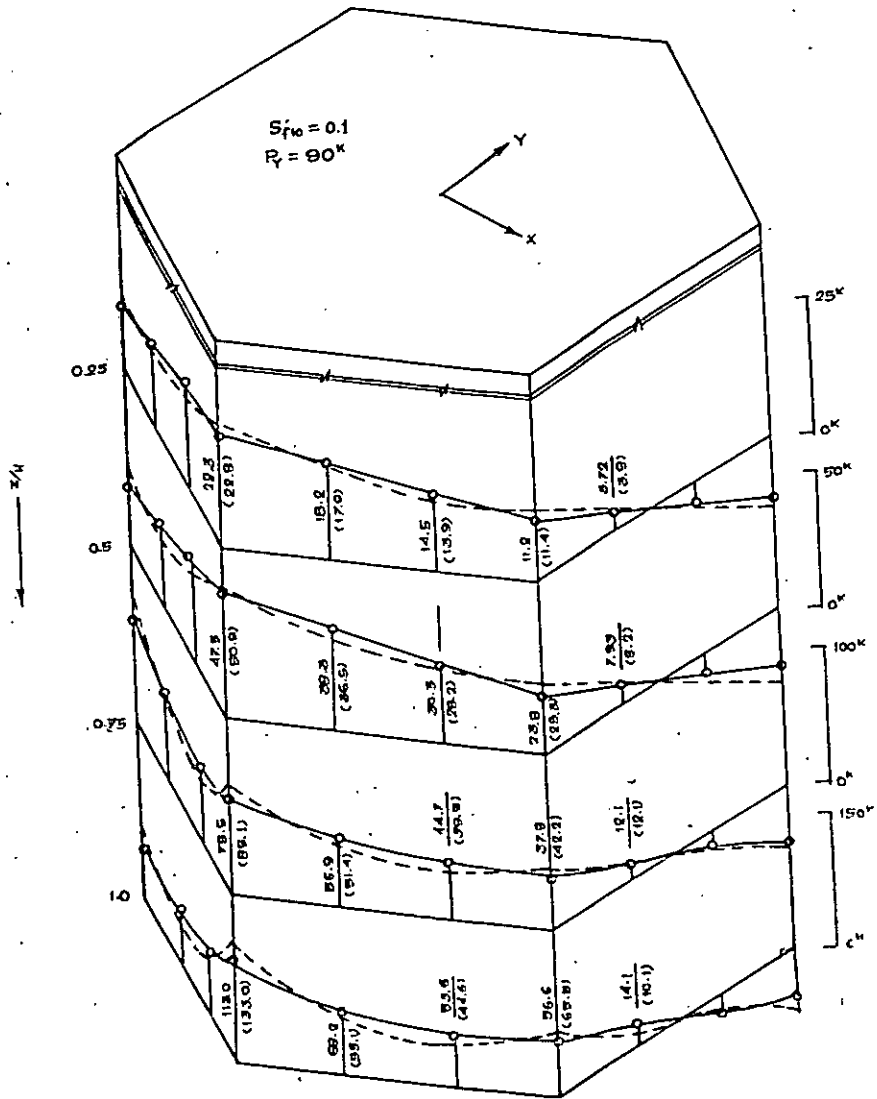


Fig.4.4 Shear-lag effect on hexagonal tubular structure (Values within parenthesis from space frame analysis)



Continuous
medium method

Space frame
analysis

Fig. 4.5 Shear-lag effect on hexagonal tubular structure
(Values within parenthesis from space frame analysis)

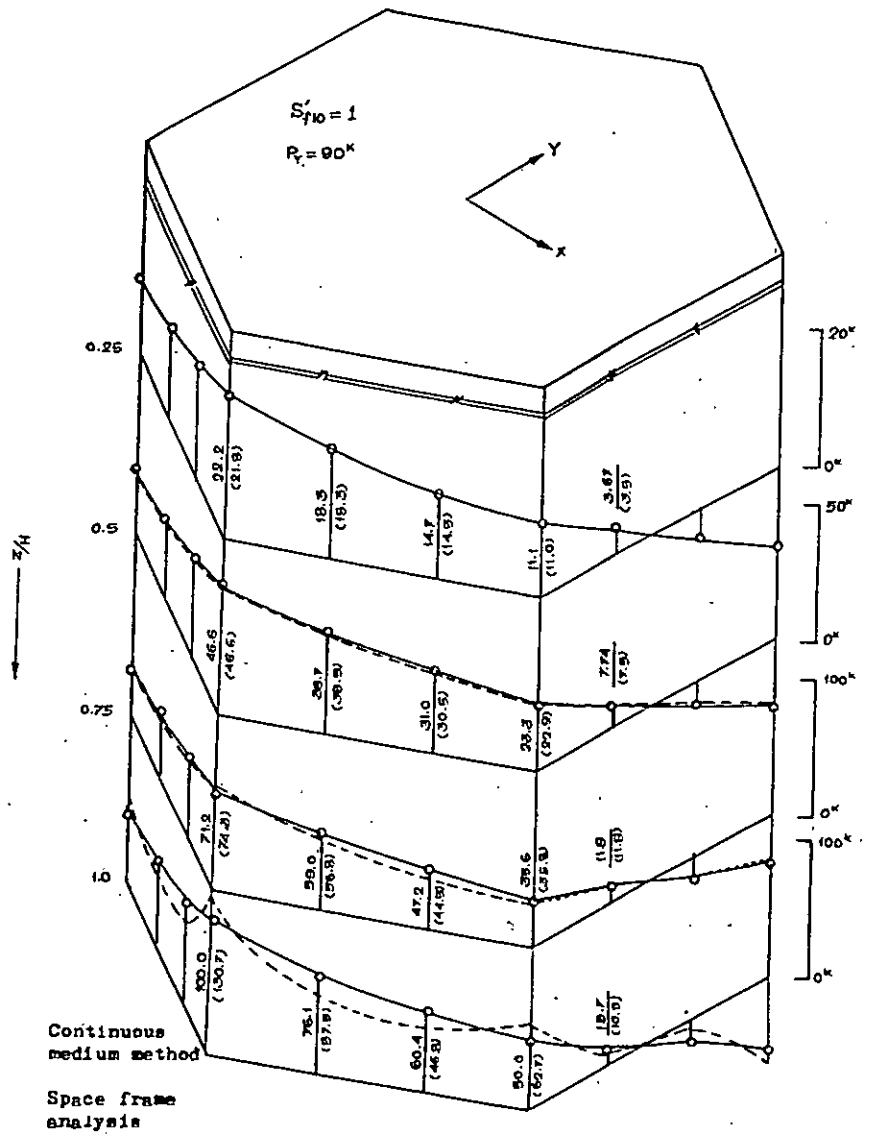


Fig.4.6 Shear-lag effect on hexagonal tubular structure
(Values within parenthesis from space frame analysis)

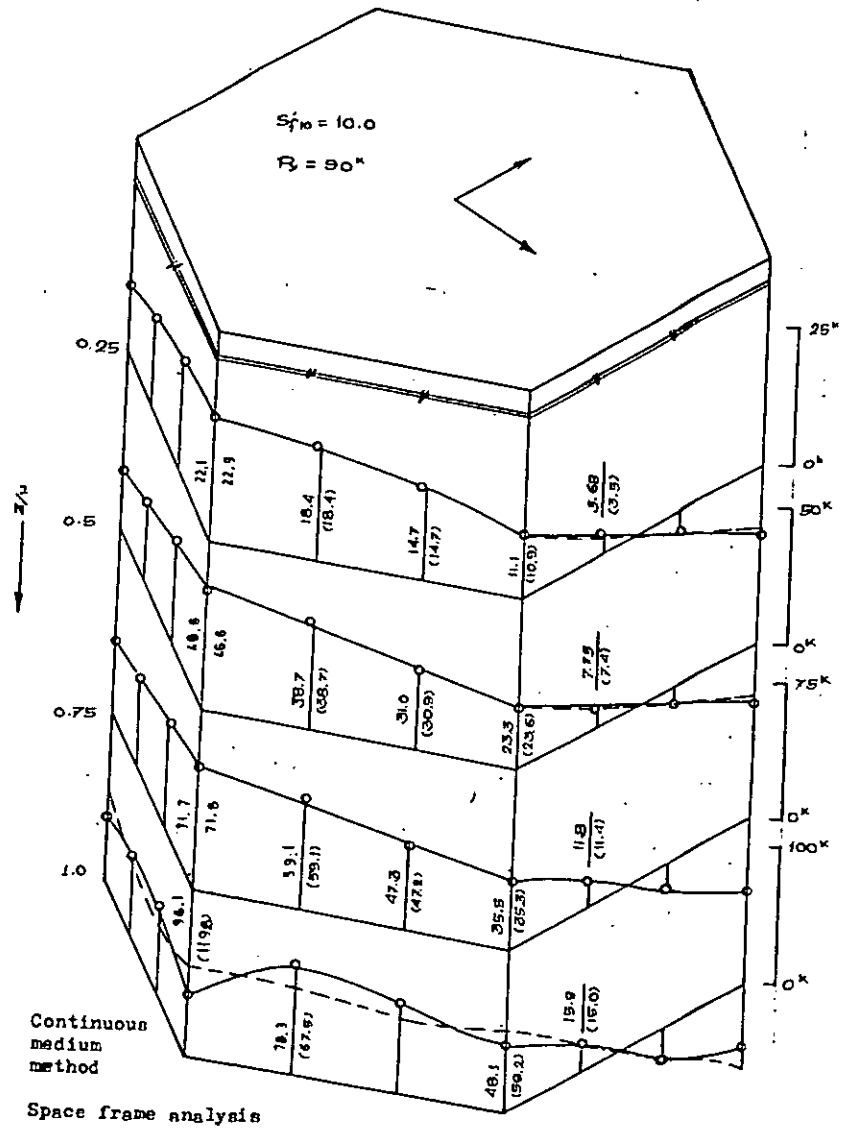


Fig. 4.7 Shear-lag effect on hexagonal tubular structure
 (Values within parenthesis from space frame analysis)

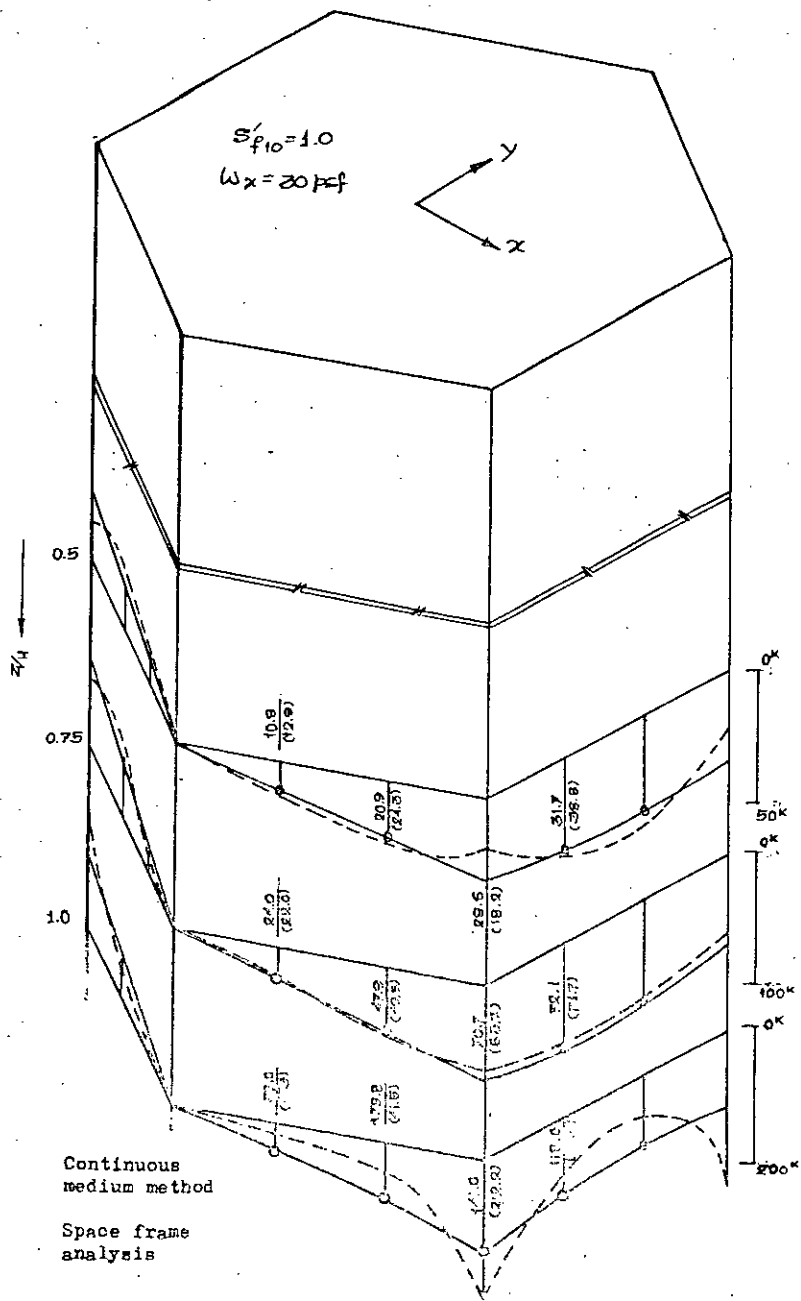


Fig. 4.9 Shear-lag effect on hexagonal tubular structure
 (Values within parenthesis from space frame analysis)

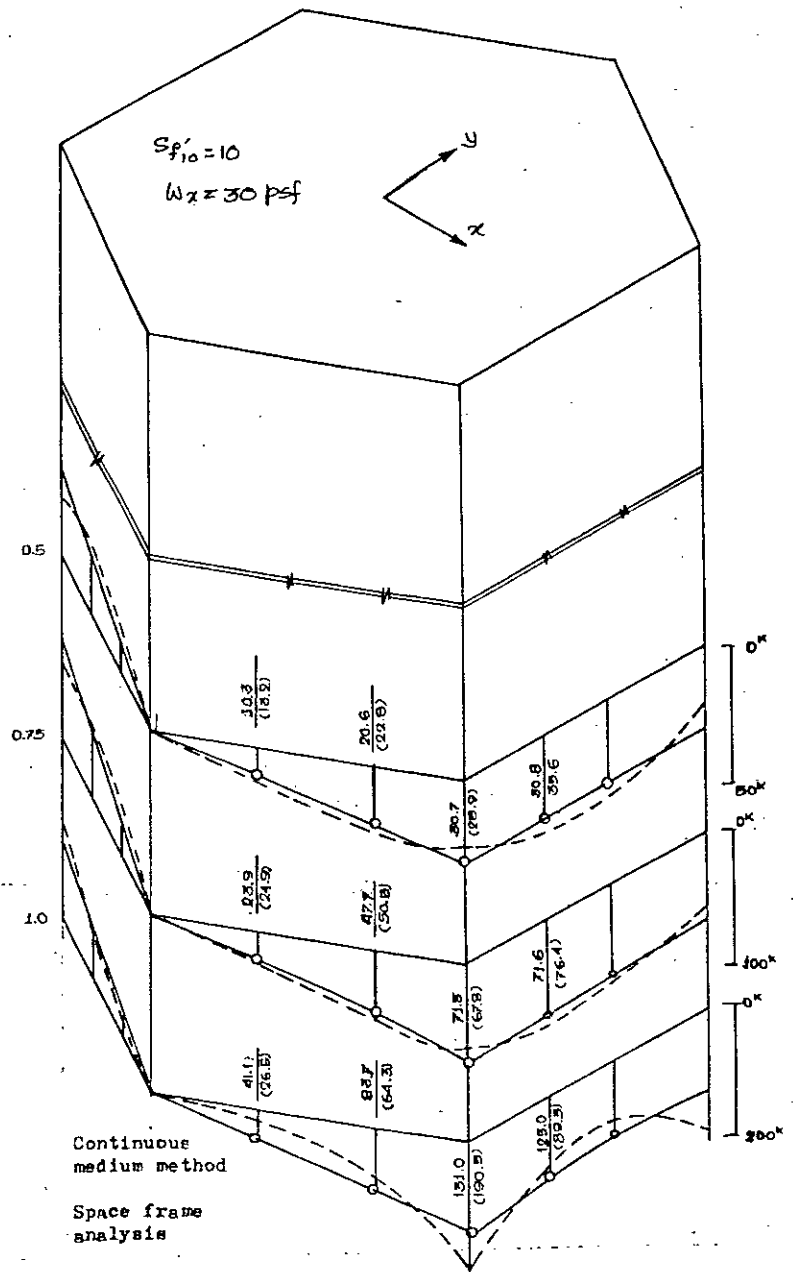
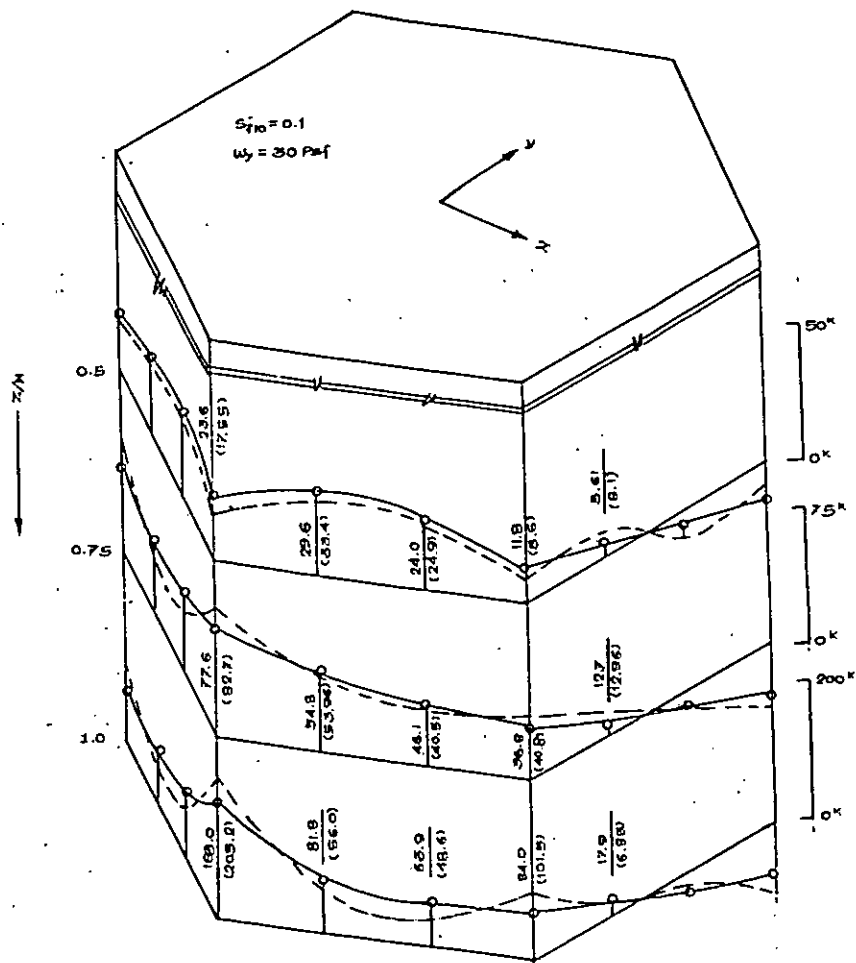


Fig. 4.10 Shear-lag effect on hexagonal tubular structure
 (Values within parenthesis from space frame analysis)



Continuous
medium method

Space frame analysis

Fig. 4.11 Shear-lag effect on hexagonal tubular structure
(Values within parenthesis from space frame analysis)

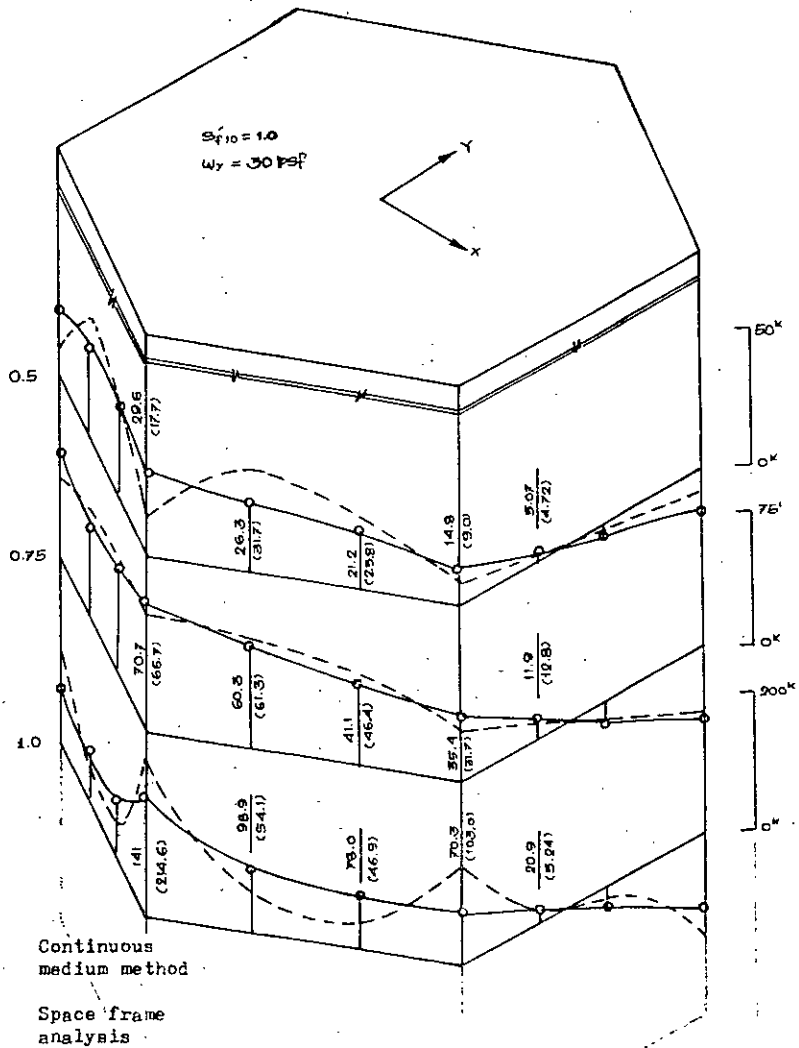


Fig.4.12 Shear-lag effect on hexagonal tubular structure
 (Values within parenthesis from space frame analysis)

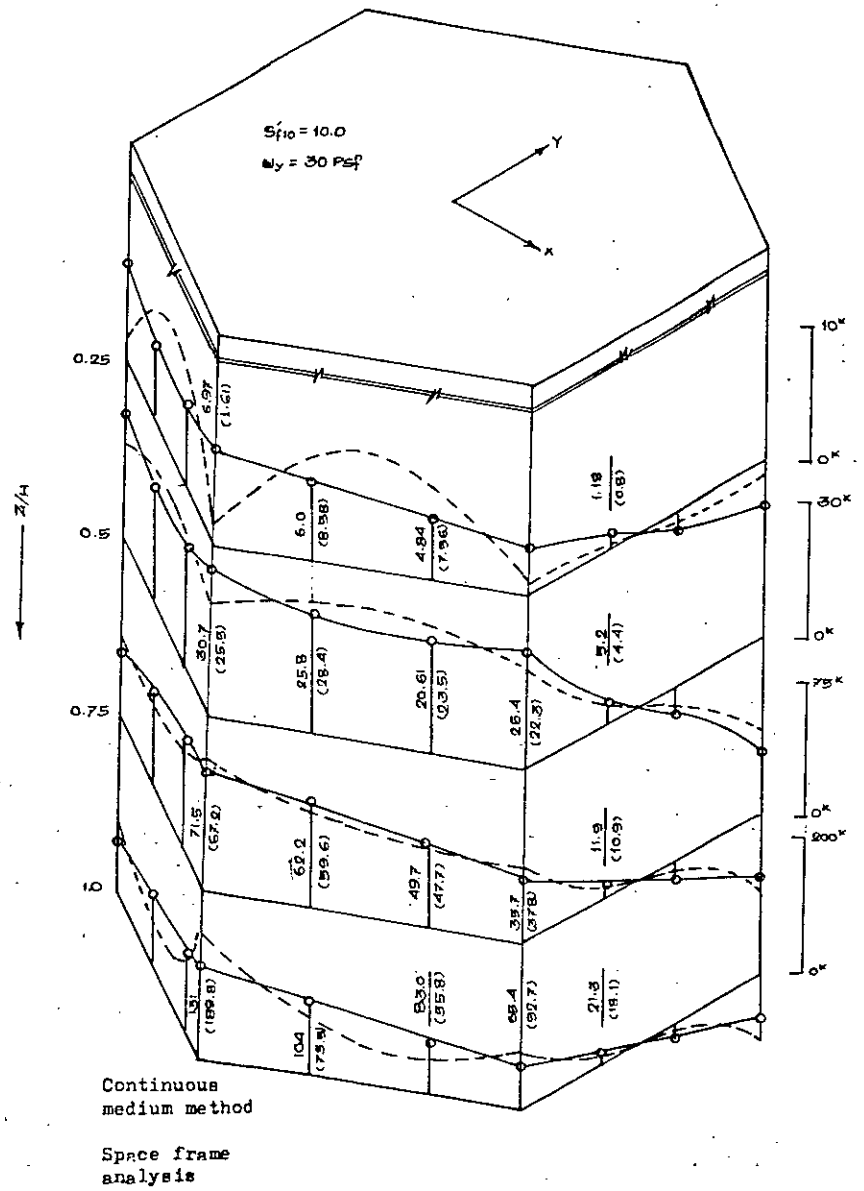


Fig.4.13 Shear-lag effect on hexagonal tubular structure
 (Values within parenthesis from space frame analysis)

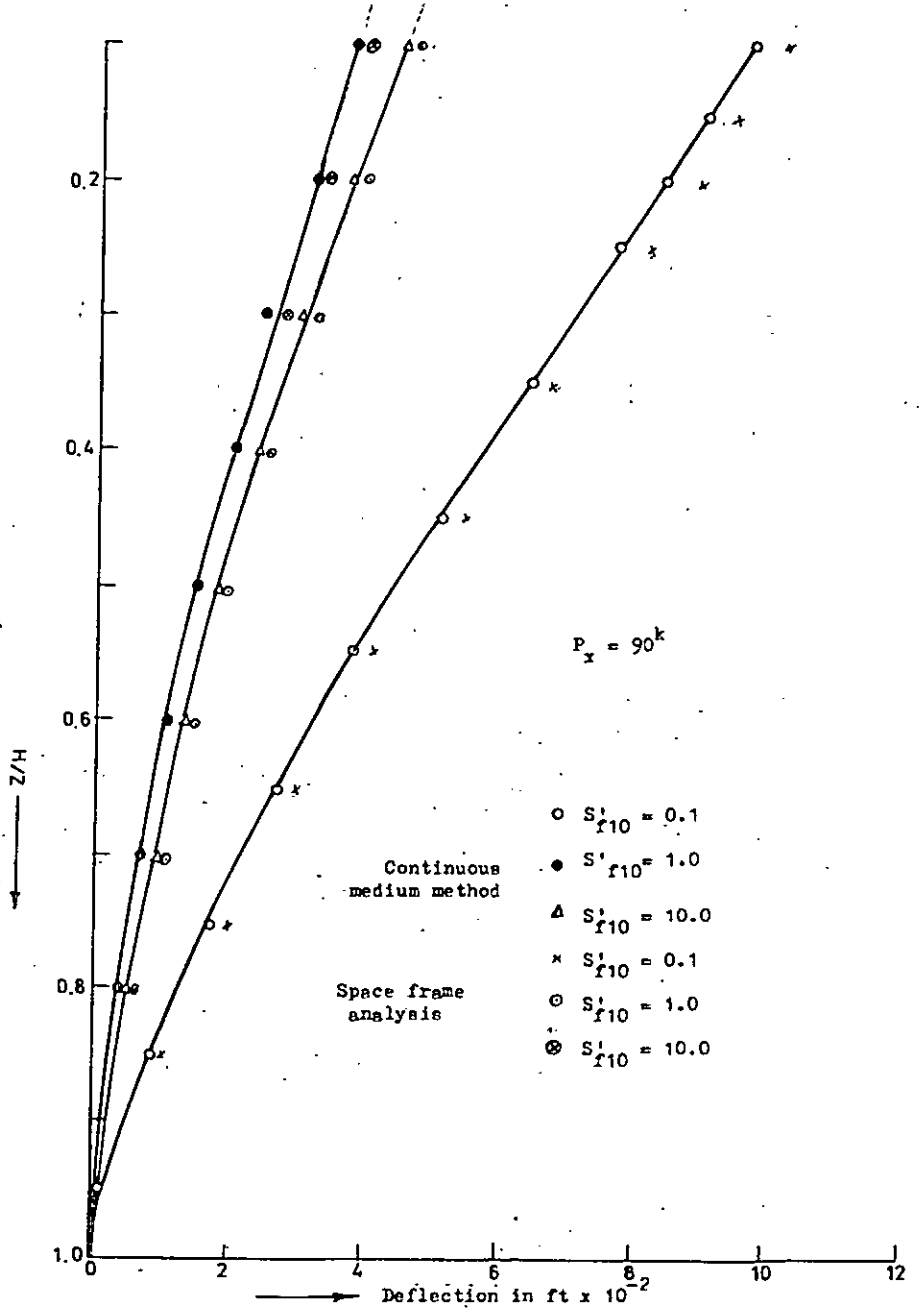


Fig. 4.14 Deflected shape of hexagonal tubular structure

$P_y = 90^k$

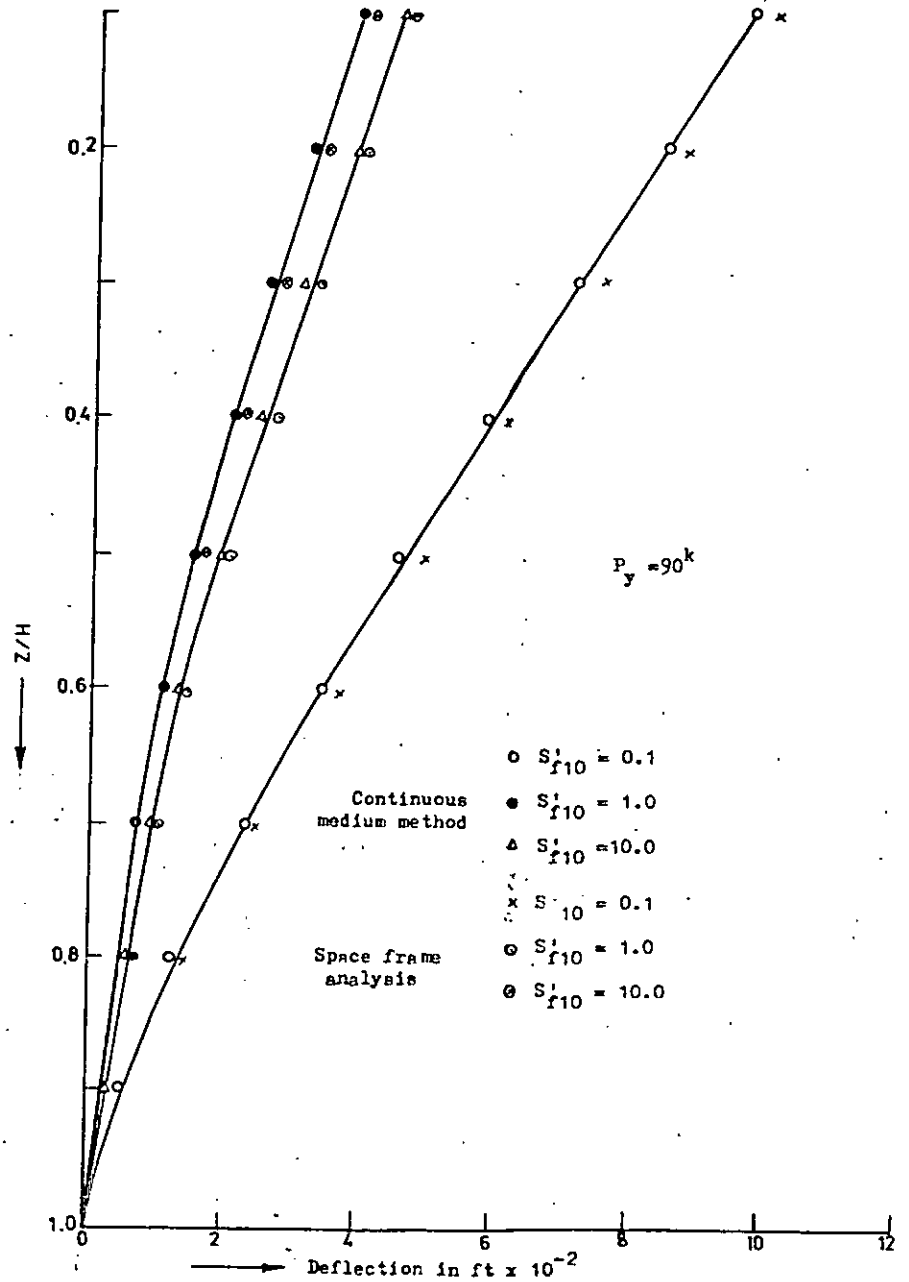


Fig. 4.15 Deflected shape of hexagonal tubular structure

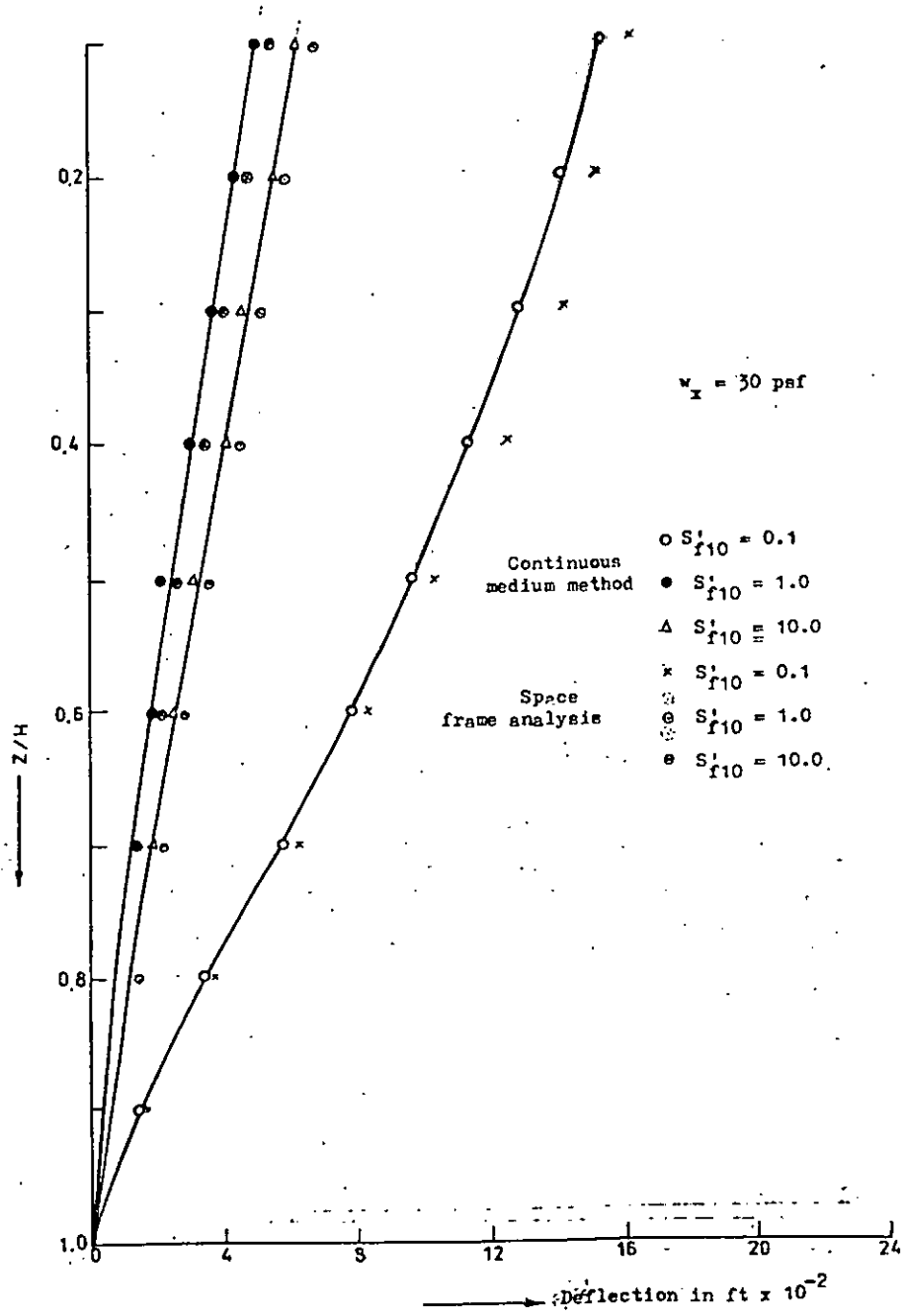


Fig. 4.16 Deflected shape of hexagonal tubular structure

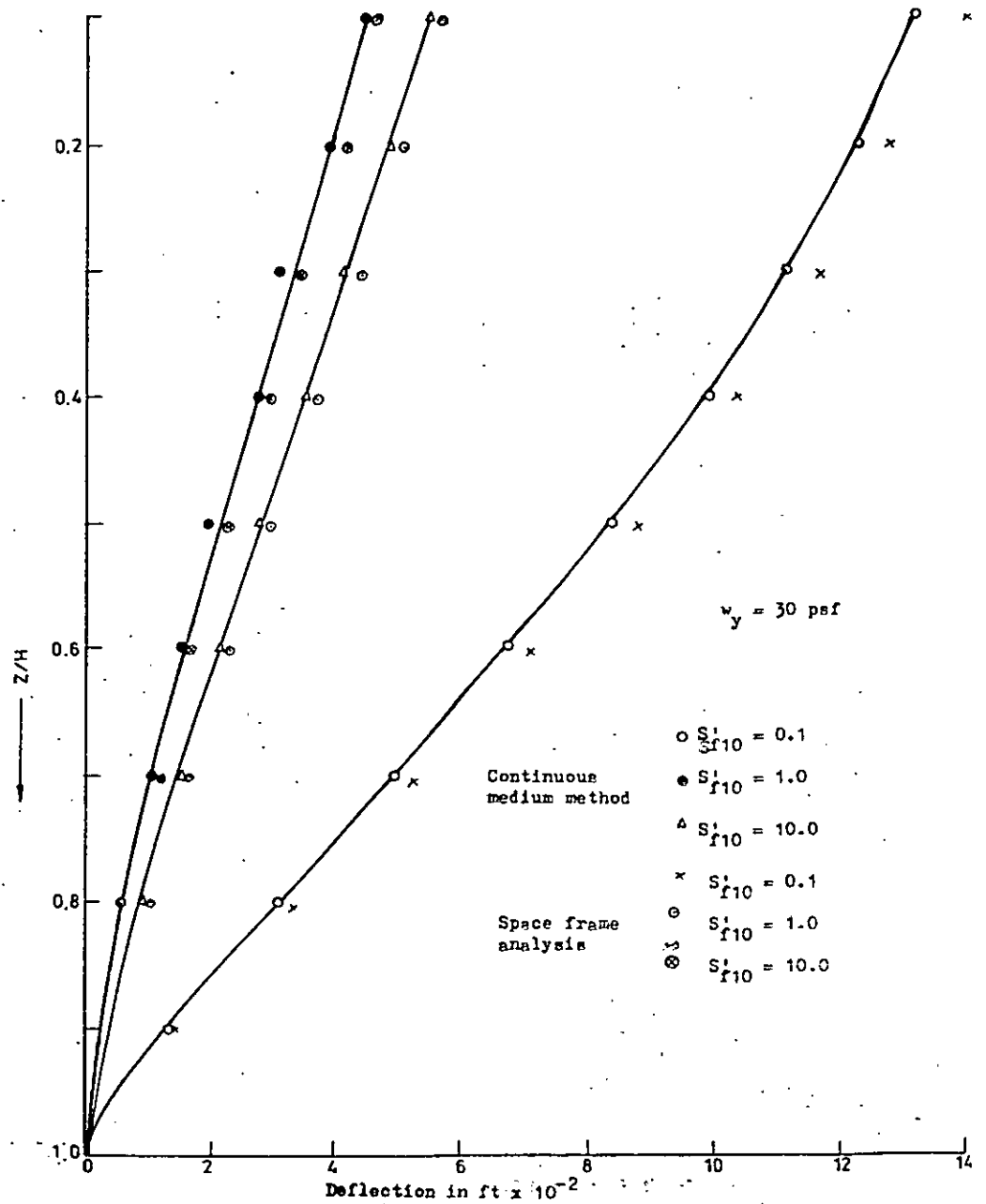


Fig. 4.17 Deflected shape of hexagonal tubular structure

CHAPTER 5

CONCLUSIONS AND RECOMMENDATIONS FOR FURTHER STUDY

5.1 Conclusions

Based on analyses of a hexagonal tubular structure with different stiffness parameters and under different loading conditions the following conclusions may be drawn:

(a) Stresses

The values of axial forces in columns for the top half of the structure obtained from the continuous medium method are almost the same as those obtained from space frame analysis for values of stiffness factors (S'_{f10}) ranging from 0.1 to 10. At the base, the maximum difference between two methods is 26% for $S'_{f10} = 0.1$ for point load applied at the top. For uniformly distributed load this variation is also at the base and in this case it is 33% for $S'_{f10} = 0.1$.

For uniformly distributed load the values of the column axial loads are less for the corner columns than the columns in between from top of the building down to $z/H = 0.5$.

The values obtained for $S'_{f10} = 10$ by continuous medium method agree very well with those obtained from the space frame analysis. The effect of shear-lag is negligible for $S'_{f10} = 10$ and its effect increases with the decrease of stiffness factor.

(b) Deflections

The deflected shapes of the structure obtained from the two methods are almost the same. The space frame analysis gives higher deflections than those obtained from continuous medium method for small values of stiffness factor. But for larger stiffness factors e.g. $S_{f10}^1 = 10.0$ the deflections are almost equal for both the cases.

Since the computer time required for continuous medium method is about 1/30, and the storage required is 1/20 of those required in space frame analysis the continuous medium approach provides a very convenient method for preliminary analysis of hexagonal tubular structures.

5.2 Recommendations for Further Study

In this study, the method is used to analyze a single tube i.e. the structure is singly connected. The method can be extended for analysing a bundled tube structure i.e. multiply connected plan form. The torsion in the beam has been neglected. A more general method may be developed including torsional effect in the connecting media.

From the series of analysis of shear-lag effect on the tubular structure, a series of influence curves may be drawn for different stiffness factor from 0.1 to 10.0.

REFERENCES

1. Ast, P.F., and Schwaighofer, J., "Economical Analysis Large Framed - Tube Structures", Building Science, Vol. 9, 1974, pp. 73-77.
2. CB, Volume, "Structural Design of Tall Concrete and Masonry Buildings", Council of Tall Buildings and Urban Habitat, Monograph, ASCE, New York, 1978.
3. Coull, A., and Bose, B., "Simplified Analysis of Frame - Tube Structures", Journal of the Structural Division, ASCE, Vol. 101, No. ST11, Proc. Paper 11696, Nov. 1975 pp. 2223-2239.
4. Coull, A., and Subbedi, N.K., "Framed Tube Structures for High-rise Buildings", Journal of the Structural Division, ASCE, Vol. 97, No. ST8, Proc. Paper 8301, August, 1971, pp. 2097-2105.
5. Coull, A and Subedi, N.K., "Hull-core Structures Subject to Bending and Torsion", Proceeding of the 9th Congress International Association for Bridge and Structural Engineering, Amsterdam, the Netherlands, May, 1972, pp. 613-632.
6. Coull, A, and Ahmed, A., "Deflections of Framed Tube Structures" - Journal of the Structural Division, ASCE, Vol. 104, No. ST5, Proc. paper 13724, May 1978, pp.857-862.
7. Choudhury, J.R., "Analysis of Plane and Spatial Systems of Interconnected Shear Walls", Ph.D. Thesis, University of Southampton, U.K., 1968.
8. Chowdhury, M.R., "Three Dimensional Analysis of Tall Building with Shear Walls and Columns of Non-Uniform Cross-section", M.Sc. Thesis, Bangladesh University of Engineering and Technology, September, 1983.

9. Chan, Paul, C.K., "Analysis of Framed-Tube Structures", Ph.D. Thesis, McMaster University, Hamilton, Ontario, Canada, 1973.
10. Chan, Tso and Heidebrecht, "Effect of Normal Frames on Shear Walls", Building Sci. Vol. 9, pp. 197-209, Pergamon Press 1974.
11. D.A. Foutch and P.C. Chang, "A Shear Lag Anomaly", Journal of the Structural Division, ASCE, Vol. 108, No. ST7, Proc. Paper 17194, July 1982.
12. Fintel, M., "Hand Book of Concrete Engineering", Van Nostrand Reinhold Company, Sept. 1974, N.Y.
13. Khan, A.H., "Analysis of Tall Shear Wall-Frame and Tube-Structures", Ph.D. Thesis, University of Southampton U.K., March 1974.
14. Khan, F.R., and Amin, N.R., "Analysis and Design of Framed Tube-Structures for Tall Concrete Buildings, The Structural Engineers, Vol. 51, 1973, pp. 85-92.
15. Khan, A.H., and Smith, B.S., "A Simple Method of Analysis for Deflection and Stresses in Wall-Frame Structures", Building and Environment, Vol. 11, 1976, pp. 69-78.
16. Kinh, H.Ha, Paul Fazio, and Osama Moselhi, "Orthotropic Membrane for Tall Building Analysis", Journal of the Structural Division, ASCE, Vol. 104, No. ST9, Sept., 1978, pp. 1495-1505.
17. Wolfgang Schueller, "High-rise Building Structures", 1st ed., John Wiley & Sons, Inc., New York, 1977.
18. Bari, Shafiul, "An approximate Method of Analysis of High-rise Tubular Structures" - M.Sc. Thesis, Bangladesh University of Engineering and Technology, August 1984.

THREE DIMENSIONAL ANALYSIS OF SHEAR WALL (19)

A.1 Introduction

A joint in a three-dimensional framed structure has in general three degrees of freedom; three rotations and three translations in x, y, and z directions. (Fig. A-1a). The assumption that the diaphragms in multistorey building are rigid constrains three displacements (D_1, D_2 and D_3) to be the same at all joints in one floor.

Any two or more walls which are monolithic will be referred to as wall assembly. A typical wall assembly is shown in Fig. A-1b. The structure is analysed to determine the forces resisted by different walls when horizontal forces in any direction are applied at floor levels. In addition to rigid diaphragm assumption it is assumed here that the floors do not restrain the joint rotation about the x and y axes (D_4 and D_5 in Fig. A-1a). The assumption is equivalent to considering that the diaphragm has small flexural rigidity compared with the walls and can therefore be ignored with this additional assumption, horizontal forces result in no axial forces in walls, thus vertical displacement D_6 in Fig. A-1a is zero.

With these assumptions, the analysis by stiffness method will now be performed.

A.2 One Storey Structure

Imagine that a building shown in Fig. A-1 has one storey height h and walls are fixed at the base. The displacement of the walls at floor level is completely defined if the displacements $\{D\}$ at the coordinates 1,2,3 are known at an arbitrary point O in the floor level. A horizontal force anywhere in the plane of the floor can be analysed into three components $\{F\}$ along the three coordinates.

The forces and displacements at shear center at the top of any wall assembly are related by

$$[S]_i \{q\}_i = \{Q\}_i \quad (A-1)$$

where $\{S\}_i$ is the stiffness matrix of the i th wall assembly and $\{q\}_i$ and $\{Q\}_i$ are respectively displacements and forces at three local coordinates in that assembly; they represent translation (or forces) at the shear center of the wall at floor level parallel to x and y axes and a rotation (or a couple) about z axis Fig. (A-1b).

To derive the stiffness matrix S_i , any wall AB is considered in Fig. A-2a fixed at base and free at the top. The flexibility matrix corresponding to the coordinates in Fig. A-2b of which 1^* and 2^* are parallel to the principal axes of inertia of the cross section is

$$[f^*]_i = \begin{bmatrix} h^3/3EI_v + h/Ga_{rv} \\ \\ h^3/3EI_u + h/Ga_{ru} \\ \\ \text{Elements not shown are zero} \\ \\ h-(\tan h)/GJ \end{bmatrix}_i \quad (A-2)$$

where I_u and I_v are second moments of the cross sectional area about the principal axes u and v respectively and a_{ru} and a_{rv} are reduced (effective) area of cross section corresponding to loading in vertical plane though v and u respectively. The second term in the expressions for f_{11}^* and f_{22}^* in the above matrix accounts for shear deformation, while the second term in f_{33}^* is included because the cross section at bottom of the wall is prevented. The parameter γ is given by

$$\gamma = \sqrt{GJ/EK} \quad (A-3)$$

where J is torsion constant (ft^4) and K is warping constant ($length^6$) of the cross section. If the shear deformation is ignored, the three diagonal terms in equation A-2 becomes $h^3/3EI_v$, $h^3/3EI_u$ and h/GJ .

The nondimensional elements in $[f^*]_i$ are all zero because the three coordinates are chosen through shear center and 1^* and 2^* are parallel to the principal axes of the section; a force applied through the shear center produces no twisting of the cross section further if this force is parallel to one of the principal axes, then the deflection takes place in a plane parallel to this axis.

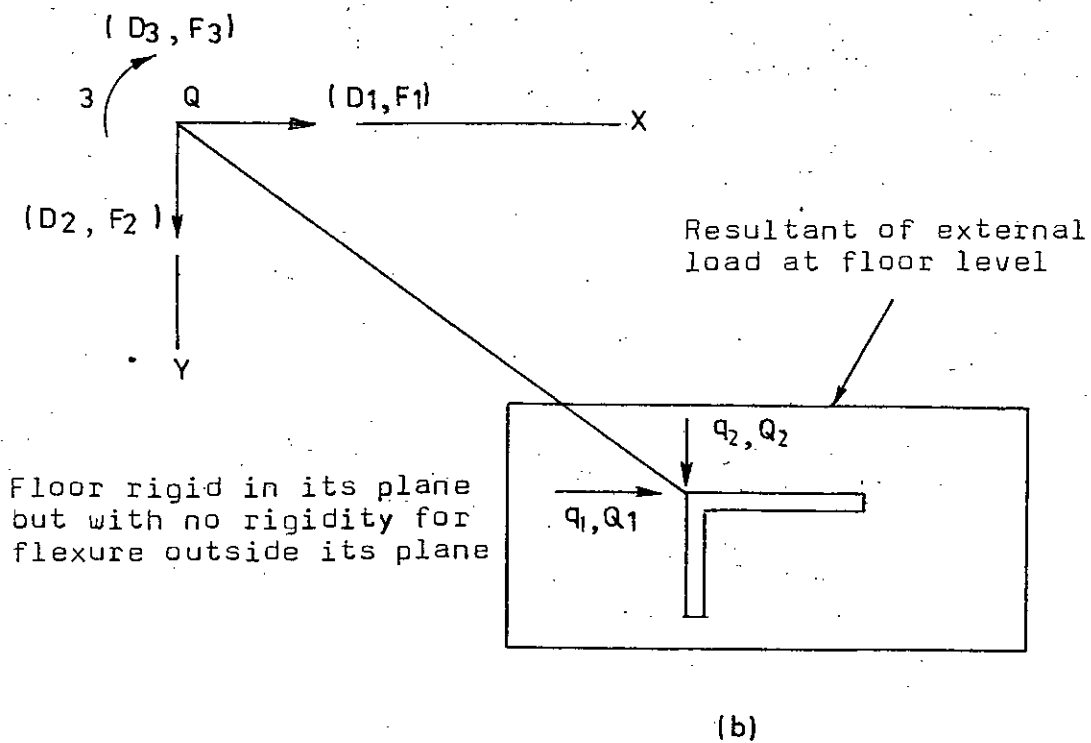
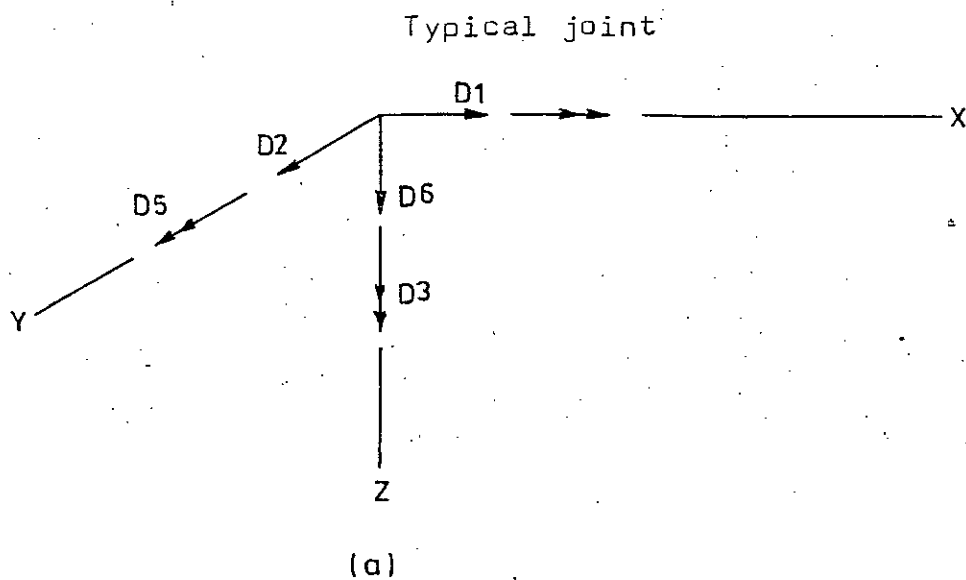
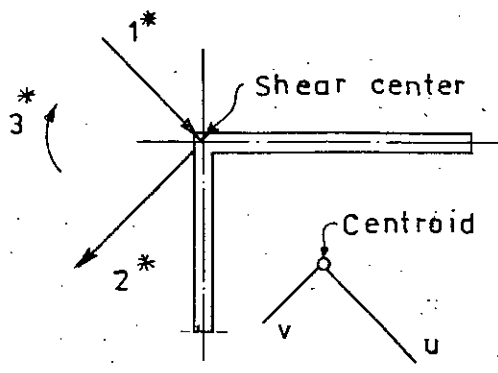
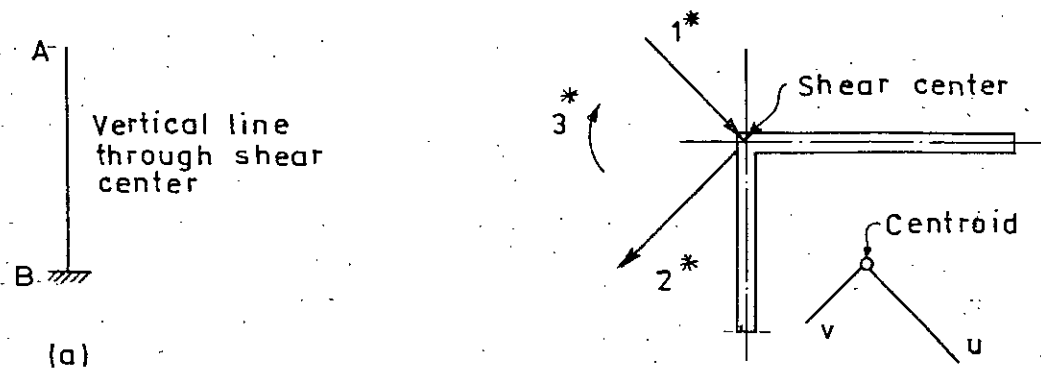
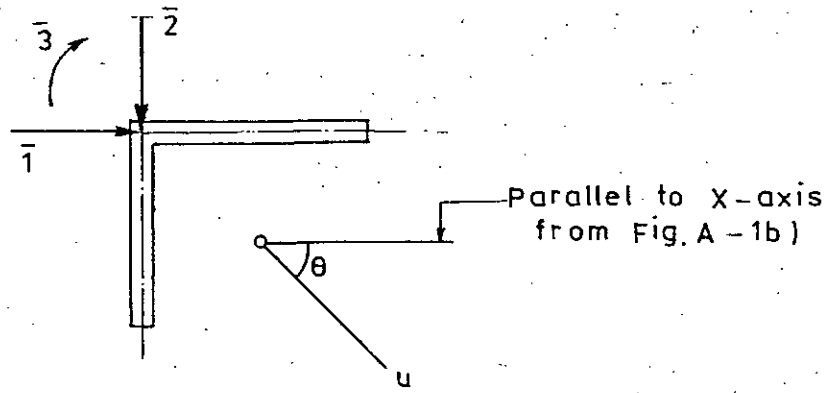


Fig. A.1 Coordinate system for analysis of single-storey shear-wall structure. (a) Degree of freedom of a typical joint in a building frame (b) Coordinate system.



u and v are centroidal principal axes. 1 and 2 are parallel to u and v through the shear center



(c)

Fig. A-2 Coordinate systems corresponding to the flexibility and stiffness matrices of a wall assembly in equation A-2, A-3 and A-4. (a) Elevation (b) Plan showing coordinates corresponding to flexibility matrix in equation A-2 (c) coordinates corresponding to matrix in equation A-4.

The stiffness matrix $[\bar{S}]_i$ corresponding to the coordinates in Fig. A-2c can be derived by inversion of $[f^*]_i$ and transformation

$$[\bar{S}]_i = \begin{bmatrix} \bar{S}_{11} & \bar{S}_{12} & 0 \\ \bar{S}_{21} & \bar{S}_{22} & 0 \\ 0 & 0 & \bar{S}_{33} \end{bmatrix}_i \quad (A-4)$$

$$\text{where } \bar{S}_{11} = E/h^3 \left[\frac{12 \cos^2 \theta}{(4+\alpha_v)} I_v + \frac{12 \sin^2 \theta}{(4+\alpha_u)} I_u \right]$$

$$\bar{S}_{22} = E/h^3 \left[\frac{12 \sin^2 \theta}{(4+\alpha_v)} I_v + \frac{12 \cos^2 \theta}{(4+\alpha_u)} I_u \right] \quad (A-5)$$

$$\bar{S}_{12} = \bar{S}_{21} = E/h^3 \left[\sin \theta \cos \theta \left(\frac{12 I_v}{4+\alpha_v} - \frac{12 I_u}{4+\alpha_u} \right) \right]$$

$$\bar{S}_{33} = GJ/h - (\tan \theta)/\gamma$$

$$\alpha_u = 12EI_u/h^2 G a_{ru} \quad (A-6)$$

$$\alpha_v = 12EI_v/h^2 G a_{rv}$$

and θ = the angle between the x and u axes.

If the shear deformation and the warping effect are ignored, the stiffness matrix in Eqn. A-4 corresponding to three coordinates in Fig. A-2c becomes

$$[\bar{S}]_i = \begin{bmatrix} 3EI_y/h^3 & \text{symmetric} & \\ 3EI_{xy}/h^3 & 3EI_x/h^3 & \\ 0 & 0 & GJ/h \end{bmatrix} \quad (A-7)$$

where I_y and I_x are the moments of inertia about axes parallel to the y and x axes through centroid and I_{xy} the product of inertia about the same axes.

The displacements $\{q\}_i$ of the i th wall are related to the floor displacement $\{D\}$ by geometry as follows.

$$\{q\}_i = [C]_i \{D\} \quad (A-8)$$

$$\text{where } [C]_i = \begin{bmatrix} 1 & 0 & -y \\ 0 & 1 & x \\ 0 & 0 & 1 \end{bmatrix} \quad (A-9)$$

where $[C]_i$ is a transformation matrix for the i th wall, and x and y are the cartesian coordinates of the shear center of this wall Fig. (A-1b). The transpose of this matrix relates the forces $\{Q\}_i$ to equivalent forces $\{F\}_i$ at the $\{D\}$ coordinates

$$\{F\}_i = [C]_i^T \{Q\}_i$$

The stiffness matrix of the i th wall corresponding to the $\{D\}$ coordinates is

stiffness but behaves like a diaphragm, the load or moment resisted by each wall of that wall assembly can be calculated by above method.

It is found that the forces or moment resisted by each wall $\{Q\}_i$ is proportional to the moment of inertia of the wall about the global axis of the wall assembly. Thus

$$Q_{x,i} = \frac{I_{y,i}}{\sum_{i=1}^m I_{y,i}} P_x,$$

$$Q_{y,i} = \frac{I_{x,i}}{\sum_{i=1}^m I_{x,i}} P_y$$

where m is the total no. of wall in that wall assembly and $I_{y,i}$ and $I_{x,i}$ are the moments of inertia of the i th wall about y and x axes which are the global axes of the assembly.

Similarly the moment resisted by each wall can be shown as

$$m_{y,i} = \frac{I_{y,i}}{\sum_{i=1}^m I_{y,i}} M_y$$

$$m_{x,i} = \frac{I_{x,i}}{\sum_{i=1}^m I_{x,i}} M_x$$

where M_x and M_y are external moments about x and y axis and $m_{x,i}$ and $m_{y,i}$ are moments resisted by i th wall about x and y axes respectively.

APPENDIX-B

SPACE FRAME PROGRAM

B.1 Introduction

The computer program presented in this appendix is based on the theory, the stiffness analysis of space frame. The sign convention used in this analysis is a right handed system of orthogonal coordinate axes (Fig. B-1) for both the local member axes and reference axes of the structure. The axes shown in Fig. B-1 indicate the positive senses of the right handed coordinate system. This program accepts data that describes the geometry and loading of a space frame and solves for the joint displacements at each joint and the member end actions of each member. Continuity is assumed at each internal joint of a space frame, and no special members are permitted in this program.

B.2 Numbering Scheme

The structure is first sketched and the joints and members numbered. A distinct number is given to each joint and member starting with the integer 1 and numbering sequentially. The number assigned to a particular joint or member is arbitrary.

The computer program assigns six displacement designations for each unstrained joint of the space frame. These numbers are assigned for a particular joint in the order indicated in Fig. B-1. The single arrows in Fig. B-1 represent translations

and double arrows represent rotations. Displacements designations are assigned only for unrestrained displacements of the joint and are assigned sequentially based on the order in which the joint coordinate data is entered.

B.3 Member Load Sign Convention

The computer program calculates fixed end shears and moments due to concentrated and uniform loads applied to a member. The load must be applied normal to one of the principal axes of inertia of the member and must pass through the shear center of the cross section. The sign convention of entering member loads is illustrated in Fig. B-2. Load P in Fig. B-2 lies in the $x_m - y_m$ plane of the member axes, and is positive as shown. Positive and negative shear angles that the loads make with normal are indicated in Fig. B-2. The components of member end displacements and actions are numbered in Fig. B-2 in sequence in which the member stiffness matrix is completed by computer.

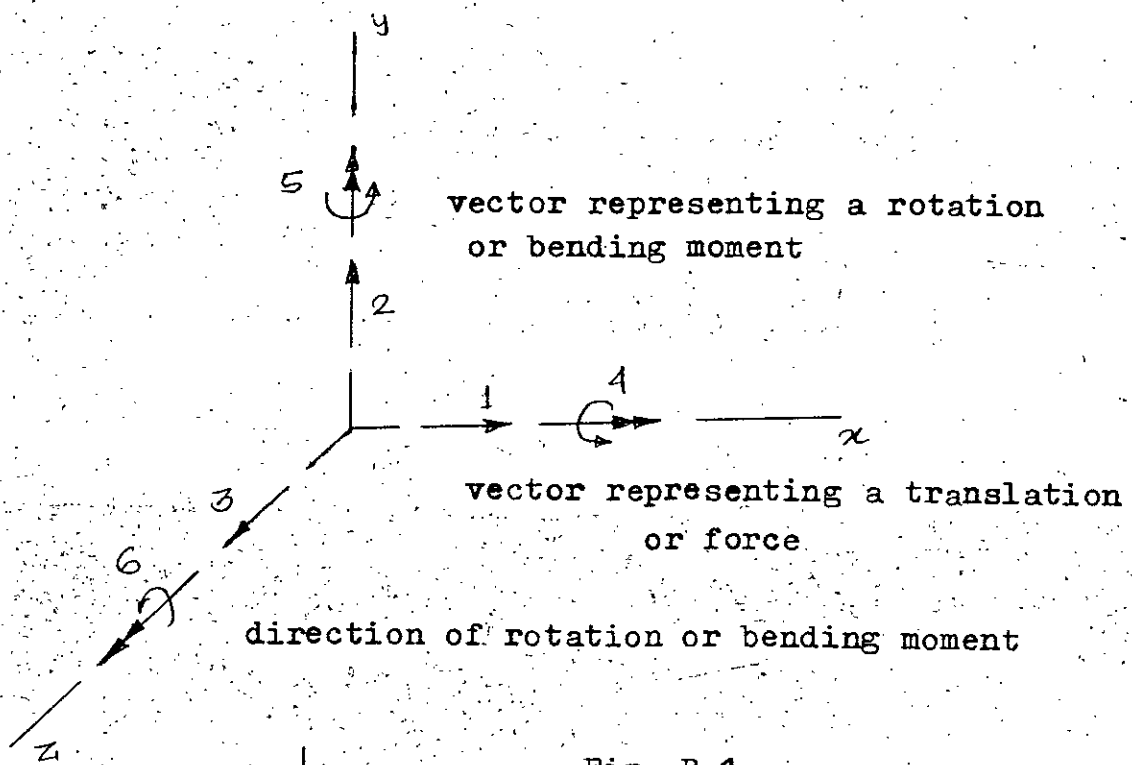


Fig. B-1

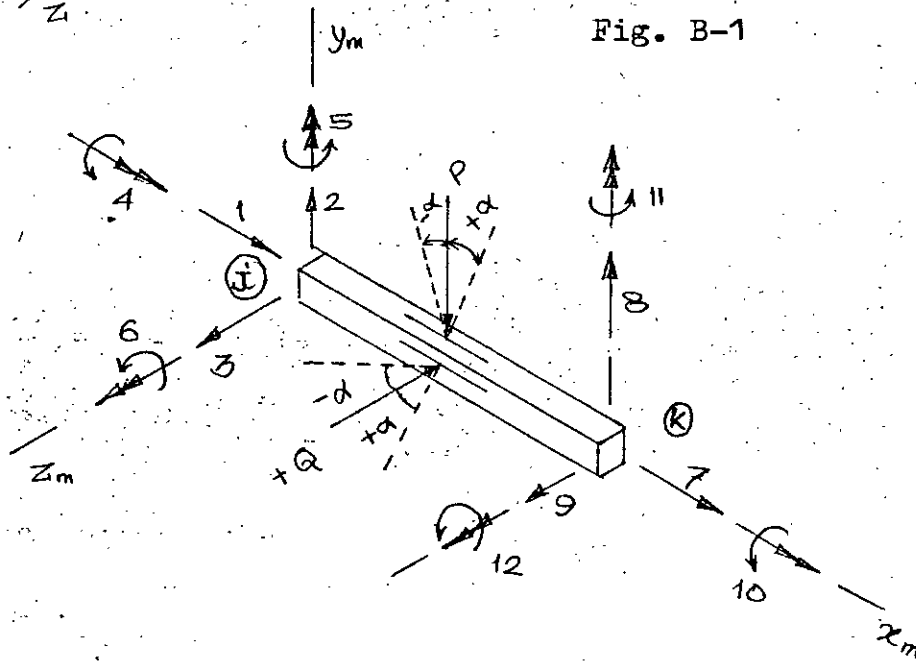


Fig. B-2

TABLE B.1
STRUCTURE DATA

Identifiers name used in program	Data description
KODE	The letter 'S' for structure card
M	Number of members in structure
NJ	Number of joints in structure
NL	Number of loading conditions for this problem
MUD	The half-band width of the stiffness matrix. If this value is unspecified or specified to small, the program will correct it at the cost of little computing time
EN	Global modulus of elasticity for the problem (k/in ²)

TABLE B.2

JOINT DATA

Identifier name used in program	Data description
KODE	The letter 'J' for joint data card
J	The joint number of this joint
IXT	x coordinate translational restraint of this joint. It is kept blank if this joint is unrestrained in x direction 'J' is placed in this column if this joint is restrained in x direction.
IYT	Same as IXT above, except in Y direction
IZT	Same as IXT above except in Z coordinate direction
IXR	Rotational restraint of this joint in x coordinate direction. It is kept blank if joint is unrestrained in x coordinate direction '1' is placed in this column if this joint is restrained in x coordinate direction.
IYR	Same as IXR except in Y coordinate direction
IZR	Same as IXR except in Z direction
XCOORD	X coordinate of joint (ft)
YCOORD	Y " " " (ft)
ZCOORD	Z " " " (ft)

TABLE B.3

MEMBER DATA

Identifier name used program	Data description
KODE	The letter M for member data
I	Member number
J	Joint number of end j of member
K	Joint number of end K of member
MT	Member type. Column is kept blank if space frame member or '1' is placed if space truss member
QIX	Moment of inertia about member x axis (in ⁴)
QIY	Moment of inertia about member y axis (in ⁴)
QIZ	Moment of inertia about member Z axis (in ⁴)
QA	Crosssectional area of member (in ²)
G	Shear modulus of elasticity (k/in ²)
SI	Angle of roll in degrees
ISI	If the angle of roll is specified for YZX, the column is left blank. If specified for rotation ZYX, '1'
E	Modulus of elasticity of this member

TABLE B.4
MEMBER LOAD DATA

Identifier name used in program	Data description
KODE	The letter 'L' for load data card.
IB1	Member no. of this member.
IB2	Plane of loading. If the load lies in the member axis x_m - y_m . Place the column is left blank. If load lies in member axis x_m - z_m plane 'L' is placed in this column.
AB1	Value of load k/ft if uniform load is specified; kips if a concentrated load is specified
AB2	Distance of joint j of member to beginning of load (ft)
AB3	Distance from joint j of member to termination of load (ft)
AB4	The angle the load makes with a normal line in degrees

TABLE B.5
JOINT LOAD DATA

Identifier name used in program	Data description
KODE	The letter P for joint load card
IB1	The joint number
AB1	Applied force in x direction at this joint (kips)
AB2	Applied force in y direction at this joint (kip)
AB3	Applied force in z direction
AB4	Applied moment about x axis at this joint (kft)
AB5	Applied moment about y axis (kft)
AB6	Applied moment about z axis (kft)

DUMMY LOAD DIVIDER CARD

KODE	The letter 'N' indicate termination of this loading condition and the beginning of a new loading condition. The letter 'E' to terminate the last loading condition.
------	---

TABLE B.7
PROGRAM TERMINATION CARD

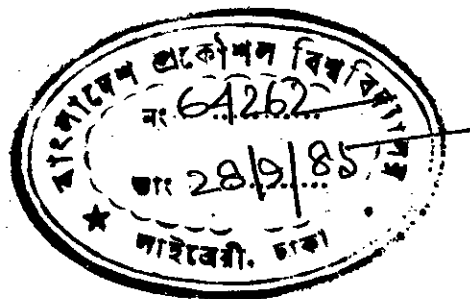
Identifier name used in program	Data description
KODE	The letter 'Q' to tell the program to quit execution. This is the last card in data deck

8.4 Preparation of Input Data

Preparation of input data for this problem should be accomplished in the following sequence:

1. The structure is sketched and the joints and members are numbered, remembering to observe the geometry of the structure in order to determine the joint sequence that will keep the half-band width of the stiffness matrix as narrow as possible.
2. A reference coordinate system is established and the joints are labelled with proper coordinate values.
3. The different load cases to be considered is defined.

The FORTRAN code of this program is given in Appendix B-2.



APPENDIX-C

(Listing of computer program of continuous medium method and space frame analysis is presented in separate cover)